



**NATIONAL UNIVERSITY OF
SCIENCE AND TECHNOLOGY
POLITEHNICA BUCHAREST**
Doctoral School of Biotechnical Systems Engineering



SUMMARY DOCTORAL THESIS

Dynamics of multibody systems in a gravitational field

**PhD supervisor,
Prof.univ.dr.eng. Ion Stroe**

**PhD student,
Eng. Sandra-Elena Nichifor**

BUCHAREST 2023

Table of contents

Introduction	3
Chapter 1	5
Multibody systems	5
Chapter 2	6
The study of kinematics and dynamics of bodies systems	6
Chapter 3	7
Modeling and simulation of a serial manipulator with 6 degrees of freedom	7
3.1. Direct kinematics	7
3.2. Inverse kinematics	8
3.3. Jacobian	10
3.4. The dynamic model of a serial manipulator with six degrees of freedom	11
3.5. Trajectory planning of a serial manipulator	12
3.6. Case study	12
3.7. Conclusions	15
Chapter 4	16
Dynamic modeling of a parallel manipulator	16
4.1. Kinematic analysis of the Stewart platform	16
4.2. The dynamic equations of the Stewart platform.....	17
4.2.1. Dynamic analysis of actuators.....	17
4.2.2. Dynamic analysis of the Stewart platform	19
4.3. Case study.....	20
4.4. Conclusions	23
Chapter 5	24
Landing of an aerial vehicle on a mobile platform	24
5.1. Dynamic model of the aerial vehicle.....	24
5.2. Landing phase.....	26
5.3. Conclusions	28
Chapter 6	29
Experimental analysis	29
Chapter 7	30
Rendezvous & docking missions	30
7.1. Trajectories in an inertial reference frame	30
7.2. Trajectories in noninertial reference frame	31

7.3.	Numerical applications according to known problems of analytical mechanics.....	32
7.4.	Motion around an orbital station	32
7.5.	Study case	33
7.6.	Conclusions	35
Chapter 8	36
	Conclusions and further developments	36
8.1.	General conclusions	36
8.2.	Original contributions.....	37
8.3.	Future research directions.....	38
Selective Bibliography	39

Introduction

The study of kinematics and dynamics of rigid body systems is very important for the development of technology, because all the results of these studies are directly applicable to specialties related to the movement of body systems: aerospace, transport. Basic knowledge of kinematics and dynamics helps to approximate and correctly calculate the relationships between the motions of objects in the system, which can make appropriate predictions about how the system will respond when subjected to external forces.

The doctoral thesis proposes the development of some mathematical models regarding the calculation of direct and inverse kinematics of some manipulators of serial type, industrial robot ABB 7600, and of parallel type, Stewart platform. Also, the dynamic model of a quadcopter was tested to achieve landing on a mobile platform with six degrees of freedom. The calculation method will use the Lagrange formalism for both inertial and non-inertial reference systems. For the rendezvous & docking missions, the known problems of analytical mechanics are considered and the comparative study of the relative motion of a satellite around an orbital station, which moves in a circular or elliptical orbit, is followed. The doctoral thesis falls within the Mechanical Field by addressing various problems specific to this field, thus carrying out systematic studies based on essential knowledge and experimental results. For this, numerical methods and simulations were used, which proved to be particularly effective tools for the mathematical calculations in this paper. The aim of the paper is focused on the dynamic modeling of multibody systems, respectively on comparative studies regarding the relative movement of a satellite with respect to an orbital station moving on a defined trajectory.

The general objective of the thesis is represented by the original contribution to the development and implementation of kinematic and dynamic models of body systems, the research methodology requiring certain methods and tools, respectively research of an extensive bibliography, conceptual modeling, numerical simulations and testing, programming languages (Matlab, Simulink, RobotStudio). To fulfill the proposed objectives, the structure of the thesis includes six main chapters, a chapter of conclusions and further developments, respectively bibliography and appendices.

The first chapter includes an overview of multibody systems, where the main basic concepts of the dynamics of body systems and kinematic models of manipulators are defined.

In Chapter 2, the general concepts of rigid bodies were exemplified and the main dynamic models used in the study of the following chapters were defined.

In Chapter 3, the direct kinematics of a serial manipulator were calculated using the Denavit-Hartenberg parameters, respectively the inverse kinematics using iterative methods, including a geometric approach. Also in this chapter, the dynamic model of the robot with six degrees of freedom was determined considering the dynamics of the speed, respectively the Jacobian, and the planning of a trajectory was defined in the RobotStudio simulation environment.

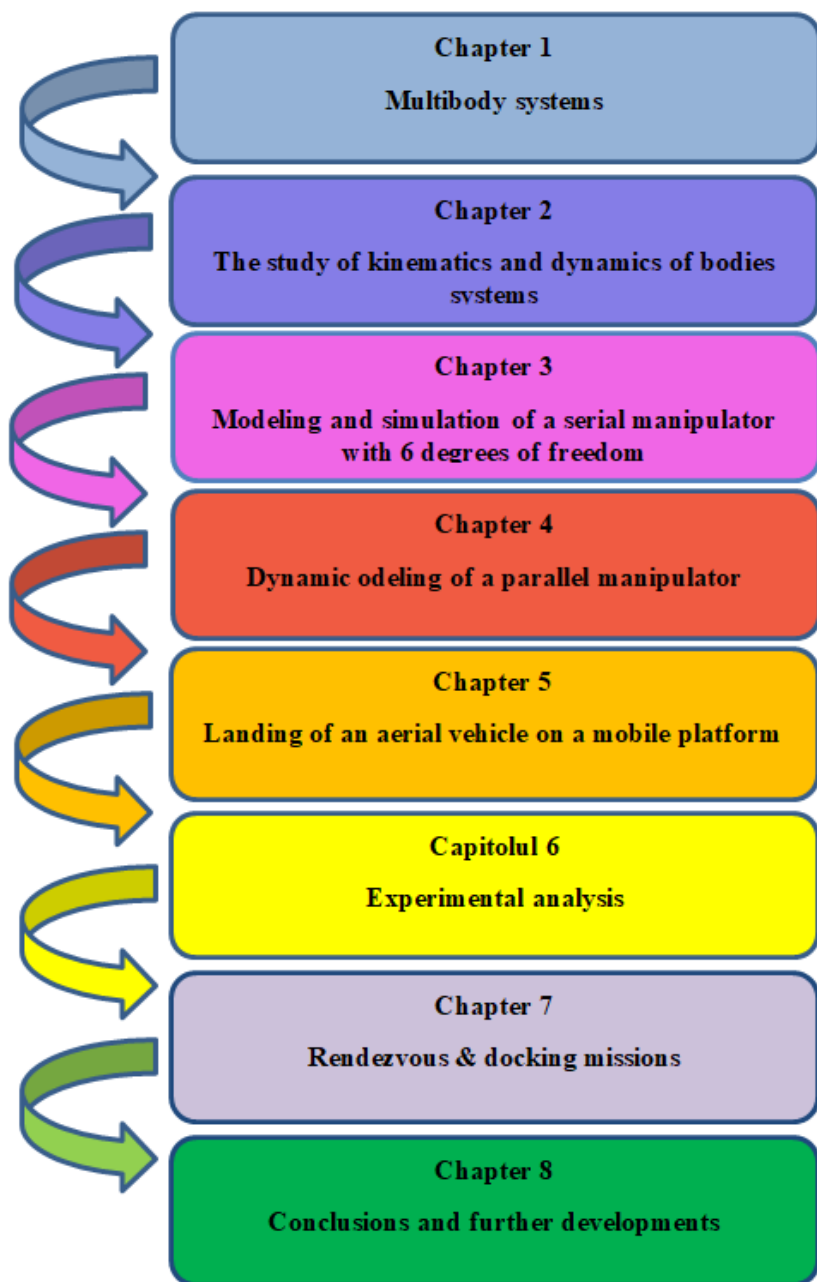
Chapter 4 presents the dynamic modeling of a six-degree-of-freedom parallel manipulator and various case studies where motions of the Stewart platform were imposed and the variation of both actuator lengths and forces with time was followed.

The importance of Chapter 5 lies in the development of the dynamic model of an aerial vehicle and its landing on a mobile platform, in this case, the one presented in Chapter 4. Furthermore, the landing time of the aerial vehicle on the platform was tracked according to the defined movement of it and the adopted control law.

Chapter 6 focuses on the experimental analysis involving the landing of an electronic drone module attached to the end effector of an ABB7600 robot on a Stewart platform.

The content of Chapter 7 focuses around the study of the relative motion of an astronaut around a much larger orbital station. The simulated case under consideration depends on the imposed trajectory of the orbital station, wherein it follows a circular path.

Chapter 8 is devoted to conclusions, personal contributions, and future directions for research and development. The diagram below represents the chapters defined in this paper.



Chapter 1

Multibody systems

This chapter emphasizes the importance of the development and diversification of mechanisms in all fields, through scientific research for the improvement of existing mechanical systems. The study of kinematics and dynamics has made significant contributions to the industrial robotics industry, thus facilitating the adaptability of robots in ever-changing environments and increasing productivity. Robotics is presented as a complex field that crosses the boundaries of traditional engineering and requires interdisciplinary knowledge in electrical engineering, systems and industrial engineering, mechanical engineering, economics, computer science and mathematics.

The importance of industrial robotics lies in the ability of robots to consistently produce quality products in a long-term production process, easing human work and improving human comfort. Robotics also has applications in areas such as space exploration and medicine, facilitating surgery and operations, as well as pharmaceutical production.

Future developments in robotics involve expansion into other theoretical areas such as nonlinear control, computational algebra, computational geometry, and intelligence in unstructured environments.

The study paper analyzes the kinematics and dynamics of rigid body systems, with an emphasis on the optimization of robots and parallel manipulators, in order to achieve complex movements and advanced technological solutions.

This chapter presents the fundamental concepts of the dynamics of systems of bodies for understanding both the motion and the behavior of bodies under the action of external forces. Within this subchapter, definitions of links, joints, chains, mechanisms, respectively degrees of freedom are considered. In this context, a definition summarizing the mechanism is given by Franz Reuleaux "the mechanism represents a set of bodies interconnected by movable joints to form a closed kinematic chain with a fixed link, designed to transform movement".

The present study aims to highlight all the basic concepts involved in the development and diversification of mechanisms with applications in more and more fields of interest, namely control, optimization, real-time simulation, route planning. In this sense, robotics will present one of the topics of interest in addressing the new research directions of the dynamics and kinematics of body systems.

Chapter 2

The study of kinematics and dynamics of bodies systems

The study of the motion of an object system can be done by two distinct types of analysis: kinematic analysis and dynamic analysis. Kinematic analysis focuses on the motion of the system without considering the forces acting on it. This involves determining the position, velocity and acceleration of the system components. In kinematic analysis, the interaction between the geometry and the motion of the system is examined without considering the forces. The elements that are driven require additional specifications within the kinematic analysis, while the other elements can be obtained using kinematic constraint equations that describe the system topology. Dynamic analysis of a system of objects focuses on the relationship and causality of the motion of the system's components, including applied external forces and moments. In this analysis, the motion of the system is not predefined and its calculation is one of the main objectives. Dynamic analysis allows the estimation of external forces that depend on the relative positions of system components, such as the forces exerted by springs, dampers, and actuators. It is also possible to estimate the external forces such as contact and friction, resulting from the interaction of the system components with the surrounding environment. During the dynamic analysis, the internal reaction forces and moments generated in the kinematic joints are also obtained, preventing relative movement in the specified directions between the connected objects.

The study of kinematics and dynamics of rigid body systems is of particular importance in the development of technology, as the results obtained are applied in a variety of fields. This chapter highlights the general concepts of rigid bodies, namely the notions of rotation matrices, kinematic quantities of rigid bodies, direct kinematics calculation, using the Denavit-Hartenberg parameters, and inverse, using the kinematic decoupling or the geometric position approach. It was also considered to present the Lagrange formalism regarding the calculation of the dynamics of rigid body systems, formulations that summarize the way in which the general equations of motion can be defined.

Chapter 3

Modeling and simulation of a serial manipulator with 6 degrees of freedom

In this chapter, the modeling and simulation of a serial manipulator with six degrees of freedom are considered. The significance of different robotic manipulators is to reach the position, respectively the required orientation of the end effector to perform different predefined tasks. In the present chapter, both the direct kinematics problem and the inverse kinematics problem will be defined. The problem of direct kinematics represents the set of all relationships that allow defining the position of the end effector according to the variables of the joints. Instead, the inverse kinematics problem ensures the determination of the coordinates of the joints that lead the end effector to the desired position and orientation. In this sense, the calculation will follow several steps: route planning, trajectory generation and control design, starting from the scheme below

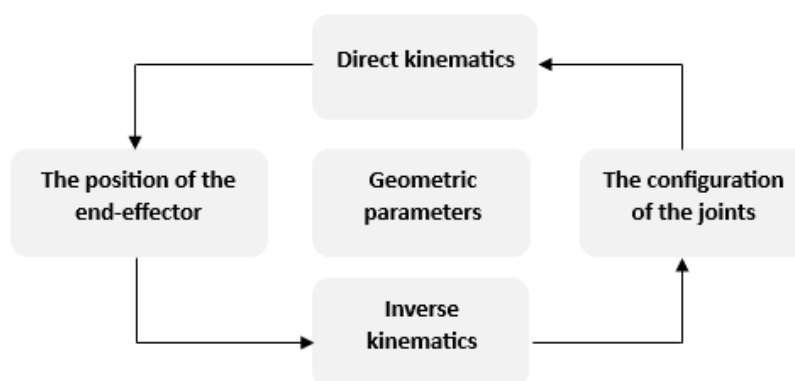


Figure 3.1 The relationship between direct and inverse kinematics

3.1. Direct kinematics

The direct kinematics problem considers determining the position and orientation of the end effector using the values of the manipulator joints.

In this sense, several possibilities for determining the position of the end effector using Cartesian coordinates, cylindrical coordinates, spherical coordinates and articulated coordinates were formulated.

In the present work, the determination of the position of the end effector of an ABB 7600 manipulator was considered, using the Denavit-Hartenberg parameters. In this sense, the transformation matrices were determined for each link of the manipulator using

$$[T_i] = \begin{bmatrix} \cos \theta_i & -\sin \theta_i \cos \alpha_i & \sin \theta_i \sin \alpha_i & a_i \cos \theta_i \\ \sin \theta_i & \cos \theta_i \cos \alpha_i & -\cos \theta_i \sin \alpha_i & a_i \sin \theta_i \\ 0 & \sin \alpha_i & \cos \alpha_i & d_i \\ 0 & 0 & 0 & 1 \end{bmatrix} \quad (3.1)$$

Knowing that the homogeneous transformation matrices between the base and each individual joint are calculated according to the formula

$$[T]_n^0 = [T]_1^0 [T]_2^1 [T]_3^2 \dots [T]_n^{n-1} \quad (3.2)$$

the following results were obtained regarding the orientation and position of the end effector

$$[R]_6^0 = \begin{bmatrix} c_1 c_{23} c_4 c_5 c_6 + c_5 s_1 s_4 c_6 - c_1 s_{23} s_5 c_6 + & s_1 c_4 c_6 - c_1 c_{23} s_4 c_6 - c_1 c_{23} c_4 c_5 s_6 - & c_1 s_{23} c_5 - c_1 c_{23} c_4 s_5 - s_1 s_4 s_5 \\ + s_1 c_4 s_6 - c_1 c_{23} s_4 s_6 & -c_5 s_1 s_4 s_6 + c_1 s_{23} s_5 s_6 & \\ s_1 c_{23} c_4 c_5 c_6 - c_1 c_5 s_4 c_6 - s_1 s_{23} s_5 c_6 - & -c_1 c_4 c_6 - c_{23} s_1 s_4 c_6 - c_{23} c_4 c_5 s_1 s_6 + & s_1 s_{23} c_5 - c_{23} c_4 s_1 s_5 + c_1 s_4 s_5 \\ -c_1 c_4 s_6 - c_{23} s_1 s_4 s_6 & +c_1 c_5 s_4 s_6 + s_1 s_{23} s_5 s_6 & \\ -s_{23} c_4 c_5 c_6 - c_{23} s_5 c_6 + s_{23} s_4 s_6 & s_{23} s_4 c_6 + c_4 c_5 s_{23} s_6 + c_{23} s_5 s_6 & c_{23} c_5 + c_4 s_{23} s_5 \end{bmatrix} \quad (3.3)$$

$$P_6^0 = \begin{bmatrix} c_1 (a_1 + a_2 c_2 + a_3 c_{23} - d_4 s_{23} - d_6 c_5 s_{23} - d_6 c_{23} c_4 s_5) - d_6 s_1 s_4 s_5 \\ s_1 (a_1 + a_2 c_2 + a_3 c_{23} - d_4 s_{23} - d_6 c_5 s_{23} - d_6 c_{23} c_4 s_5) + d_6 c_1 s_4 s_5 \\ -a_2 s_2 - a_3 s_{23} + d_6 c_4 s_{23} s_5 - d_4 c_{23} - d_6 c_{23} c_5 + d_1 \end{bmatrix} \quad (3.4)$$

$$s_x = \sin \theta_x, x = 1, 2 \dots 6$$

$$c_x = \cos \theta_x, x = 1, 2 \dots 6$$

in which the following notations were made:

$$c_{xy} = \cos(\theta_x + \theta_y), x = 1, 2 \dots 6, y = 1, 2 \dots 6$$

$$s_{xy} = \sin(\theta_x + \theta_y)$$

3.2. Inverse kinematics

Inverse kinematics is an essential field in robotics, which deals with determining the joint angles of a robotic system to achieve a specific position and orientation of the end effector. Solving the inverse kinematics problem can sometimes be difficult because it involves determining mathematical solutions to a non-linear system of equations. Although analytical methods exist for certain types of robots and configurations, in many cases exact solutions cannot be obtained in a simple way. Thus, numerical methods and iterative algorithms are often used to find approximate solutions.

Regarding the analytical methods for solving the inverse kinematics problem, a series of specialized papers highlighting different approaches are considered. Recent research was carried out in specialized work [19] in which the inverse kinematics was calculated on a manipulator that consisted of several links interconnected by seven revolutionary joints. In this case, the inverse kinematics problem was solved by using an angular coefficient of a link to represent the redundancy of the serial manipulator. The fourth joint was derived in a closed-form expression, taking into account the spherical configuration of the base. This led to the calculation of the other joints using the inverse kinematics equations.

The iterative method of inverse kinematics based on the geometry of the serial manipulator is one of the approaches chosen in this work. This method was chosen because it can obtain multiple solutions, if any, at any well-defined position and orientation. Regarding the determination of the first two joint angles of the manipulator configuration, their kinematic expressions are derived from two nonlinear trigonometric equations. The rest of the

joint angles are determined by successive substitution of the roots obtained in the kinematic expressions.

Both the positions of the end-effector are considered known, $\{P_6^0\} = \{P_x P_y P_z\}^T$, as well as the bond parameters, to determine the joint angles using inverse kinematics.

- General inverse kinematics problem

The general inverse kinematics problem consists in imposing the position and orientation of the end effector, respectively

$$[H] = \begin{bmatrix} h_{11} & h_{12} & h_{13} & P_x \\ h_{21} & h_{22} & h_{23} & P_y \\ h_{31} & h_{32} & h_{33} & P_z \\ 0 & 0 & 0 & 1 \end{bmatrix} \quad (3.5)$$

Where it was noted with h_{ij} ($i, j = \overline{1,3}$) end-effector rotation matrix components, P_x, P_y, P_z representing the final effector position components on the three axes, all of which are known.

Thus, the relation can be written

$$[T]_6^0 = [T]_1^0 [T]_2^1 [T]_3^2 [T]_4^3 [T]_5^4 [T]_6^5 = [H] \quad (3.6)$$

By means of this relationship, a system of 12 nonlinear equations with 6 unknowns is obtained, and to determine all the joints, successive multiplication with the inverse matrix of a certain transformation on both sides of the robot's kinematic equation is considered.

The first articulation is determined by multiplying the relationship (3.6) with $[T]_1^{0^{-1}}$, obtaining the value of the angle of the first joint

$$\theta_1 = \arctg \left(\frac{P_y - d_6 h_{23}}{P_x - d_6 h_{13}} \right) \quad (3.7)$$

The next step is to multiply the equation (3.6) with the inverse of the matrix $[T]_3^{2^{-1}}$, thus obtaining the value of the fourth joint

$$\theta_4 = \arctg \left(\frac{h_{13} s_1 - h_{23} c_1}{(h_{13} c_1 + h_{23} s_1) c_{23} - h_{33} s_{23}} \right) \quad (3.8)$$

As for determining the value of the fifth joint, multiply the relationship (3.6) with $[T]_4^{3^{-1}}$ and it is obtained

$$\theta_5 = \arctg \left(\frac{(h_{13} c_1 + h_{23} s_1) c_{23} c_4 - h_{33} s_{23} c_4 + (h_{13} s_1 - h_{23} c_1) s_4}{(h_{13} c_1 + h_{23} s_1) s_{23} + h_{33} c_{23}} \right) \quad (3.9)$$

The last step represents the multiplication of relationship (3.6) with the matrix $[T]_5^{4^{-1}}$, and by mathematical calculations it is obtained

$$\theta_6 = \arctg \left(\frac{-(h_{11} c_1 + h_{21} s_1) c_{23} s_4 + h_{31} s_{23} s_4 + (h_{11} s_1 - h_{21} c_1) c_4}{-(h_{12} c_1 + h_{22} s_1) c_{23} s_4 + h_{32} s_{23} s_4 + (h_{12} s_1 - h_{22} c_1) c_4} \right) \quad (3.10)$$

Considering the complex mathematical calculation regarding the determination of the angles θ_2 and θ_3 , the geometrical problem for the calculation of the two angles will be addressed next.

- Geometric approach to position for determining angles θ_2 and θ_3

Another simple method to solve the inverse kinematics is by removing the last link and keeping the first three joints of the robotic arm to determine the angle values θ_2 and θ_3 .

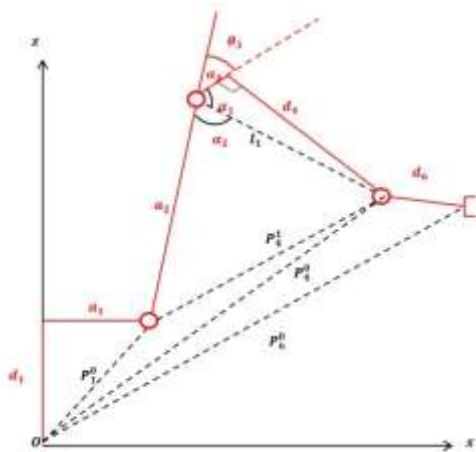


Figure 3.2 Simplified side view of the robotic arm

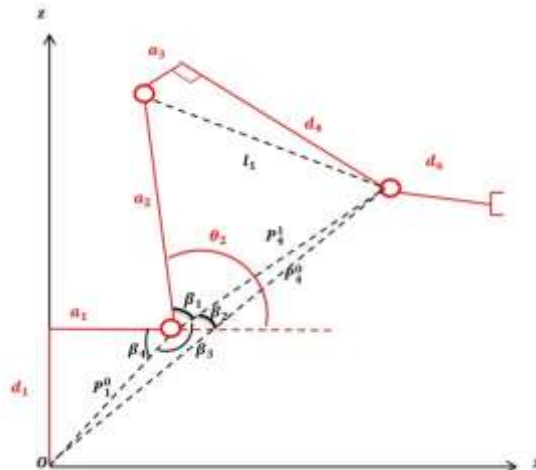


Figure 3.3 Robotic arm side view

As can be seen in *Figure 3.2*, by using trigonometric relationship certain lengths can be determined, e.g. l_1 , α_1 , where P_0^4 represents the position of the fourth joint relative to the base of the robotic arm, P_0^1 is the position of the first joint relative to the base of the robotic arm, P_4^1 represents the position of the fourth joint relative to the first joint.

Following the known mathematical calculations, the value of the third angle was determined

$$\theta_3 = \pi - \arctg\left(\frac{d_4}{a_3}\right) - \arccos\left(\frac{a_2^2 + l_1^2 - P_{14}^2}{2a_2l_1}\right) \quad (3.11)$$

Regarding the determination of the second angle, the geometric elements from *Figure 3-3* will be identified. In the first stage, the lengths corresponding to the positions of joints two and four are identified in relation to the position of the first joint of the robotic arm, finally obtaining the expression of the angle of the second joint

$$\theta_2 = \pi - \arccos\left(\frac{a_2^2 + P_{14}^2 - l_1^2}{2a_2P_{14}}\right) - \arccos\left(\frac{P_{01}^2 + P_{14}^2 - P_{04}^2}{2P_{01}P_{14}}\right) - \arctg\left(\frac{d_1}{a_1}\right) \quad (3.12)$$

3.3. Jacobian

In robot modeling and control, the Jacobian is an essential part of planning and executing trajectories, determining configurations, executing coordinated motions, deriving dynamic equations of motion, and transforming forces and torques from the end-effector to the joints.

In this sense, the ABB7600 robot that has 6 kinematic links will have the Jacobian in the form of a 6x6 matrix that can be used both for determining the angular and linear velocity of the end effector, as well as for determining the velocity of any point of the manipulator. Both linear and angular velocity will be treated separately, the angular velocity of the end effector being defined by the antisymmetric square matrix.

Using the Jacobian matrix, J , the two velocities can be described

$$\begin{aligned} \{v_k\} &= [J_{v_k}]\{\dot{q}_k\} \\ \{\omega_k\} &= [J_{\omega_k}]\{\dot{q}_k\}, \quad k = 1, 2, \dots, 6 \end{aligned} \quad (3.13)$$

where v_k is the linear velocity, ω_k is the angular velocity, J_{v_k} and J_{ω_k} represent the linear and angular velocity Jacobian matrices, \dot{q}_k represent the generalized velocity coordinates, respectively

$$\{\dot{q}\} = \{\dot{\theta}_1 \ \dot{\theta}_2 \ \dot{\theta}_3 \ \dot{\theta}_4 \ \dot{\theta}_5 \ \dot{\theta}_6\}^T \quad (3.14)$$

Considering that the ABB7600 model has six revolute joints, the formulas for determining the Jacobian matrices are defined

$$\{J_{v_i}\} = \left\{ [R]_{i-1}^0 \begin{bmatrix} 0 \\ 0 \\ 1 \end{bmatrix} \times (\{P\}_n^0 - \{P\}_{i-1}^0) \right\}, \quad n = 6, i = \overline{1,6} \quad (3.15)$$

$$\{J_{\omega_i}\} = \left\{ [R]_{i-1}^0 \begin{bmatrix} 0 \\ 0 \\ 1 \end{bmatrix} \right\}, \quad i = \overline{1,6} \quad (3.16)$$

In this subsection, the linear and angular Jacobian matrices were determined for each individual arm of the robot, taking into account those previously highlighted and the fact that

$$[R]_0^0 = \begin{bmatrix} 1 & 0 & 0 \\ 0 & 1 & 0 \\ 0 & 0 & 1 \end{bmatrix}, \quad \{P\}_0^0 = \begin{Bmatrix} 0 \\ 0 \\ 0 \end{Bmatrix} \text{ și } \{P\}_6^0 = \begin{Bmatrix} P_x \\ P_y \\ P_z \end{Bmatrix}.$$

3.4. The dynamic model of a serial manipulator with six degrees of freedom

Considering the kinematics of the manipulator described in point 3.1., in this sense the notation axis/angle is used to represent the attitude of the end effector [5]. Thus, for any rotation matrix $[R]$, a single rotation of an axis in space through an appropriate angle is considered.

The study of the dynamic model of the ABB IRB 7600 robot considers the Lagrange equations

$$\frac{d}{dt} \left(\frac{\partial L}{\partial \dot{q}_k} \right) - \frac{\partial L}{\partial q_k} = \tau, \quad k = \overline{1,6} \quad (3.17)$$

where the Lagrangian is defined as the difference between kinetic and potential energy.

Also, the mechanical system of the ABB 7600 robot depends on two assumptions

- The system is subject to holonomic constraints
- Constraint forces satisfy the principle of virtual mechanical work

Using the relation (3.17), the general form of robot dynamics can be written

$$M(q)\ddot{q} + C(q, \dot{q})\dot{q} + G(q) = \tau \quad (3.18)$$

where $M(q)$ represents the mass matrix and contains inertial forces, $C(q, \dot{q})$ represents the vector of Coriolis forces and centrifugal forces, $G(q)$ represents the vector of gravitational forces.

After determining the kinetic and potential energies, the Coriolis and centrifugal forces, and the gravitational forces, the following equation of the dynamic model of the robot was obtained

$$\left[\{J_{v_i}\}^T m_i \{J_{v_i}\} + \{J_{\omega_i}\}^T [I_i] \{J_{\omega_i}\} \right] \ddot{q} + \left[\dot{M}(q) \{\dot{q}\} - \frac{1}{2} \{\dot{q}\}^T \frac{\partial M(q)}{\partial q_k} \{\dot{q}\} \right] \dot{q} - \sum_{i=1}^6 J_{v_i}^T m_i g = \tau \quad (3.19)$$

$i = \overline{1,6}$.

3.5. Trajectory planning of a serial manipulator

Trajectory planning represents a crucial aspect of controlling serial manipulators in robotics. This involves generating collision-free and efficient trajectories for the robot's end effector to accomplish various tasks. Regarding the trajectory planning of the ABB7600 serial manipulator, a fourth-order polynomial was considered for defining the trajectory, determining angular displacement, angular velocity, and angular acceleration for a start-move-stop motion. In this regard, the initial and final joint angles were imposed.

3.6. Case study

This case study considered the mathematical modeling and kinematic analysis of an ABB IRB7600 robotic arm. It was mathematically modeled using the Denavit-Hartenberg parameters, the forward and inverse kinematics solutions being generated and implemented using Matlab software. In this developed software the motion kinematics were tested and the relevant motion was determined.

The Denavit-Hartenberg parameters of the manipulator can be found in the table below

Link	$d_i [m]$	$\theta_i [deg]$	$a_i [m]$	$\alpha_i [deg]$
1	$d_1 = 0.78$	$\theta_1 = 45$	$a_1 = 0.41$	$\alpha_1 = -90$
2	0	$\theta_2 = 30$	$a_2 = 1.075$	0
3	0	$\theta_3 = 30$	$a_3 = 0.165$	$\alpha_3 = -90$
4	$d_4 = 1.056$	$\theta_4 = -45$	0	$\alpha_4 = 90$
5	0	$\theta_5 = 30$	0	$\alpha_5 = -90$
6	$d_6 = 0.25$	$\theta_6 = 0$	0	0

Table 1 Denavit-Hartenberg parameters

This case study considers the verification and validation of the obtained relationships of the joint values following the inverse kinematics procedure. The first step was to identify the orientation and position of the end-effector

$$\{P_6^0\} = \begin{pmatrix} 0.2586 \\ 0.1336 \\ -0.4601 \end{pmatrix} \quad (3.20)$$

$$[R]_6^0 = \begin{bmatrix} -0.5227 & 0.7500 & -0.4053 \\ 0.3433 & -0.2500 & -0.9053 \\ -0.7803 & -0.6124 & -0.1268 \end{bmatrix} \quad (3.21)$$

The second step was the inverse kinematics calculation described in point 3.2., the joint values thus obtained being $\theta_1 = 45^\circ$; $\theta_2 = 29.9977^\circ$; $\theta_3 = 29.9993^\circ$; $\theta_4 = -44.9962^\circ$; $\theta_5 = 30.0036^\circ$; $\theta_6 = -0.0052^\circ$.

Following the comparative study of the calculated values of the joint angles of the robotic arm using inverse kinematics, it is observed that the described mathematical model is applicable to the ABB 7600 model.

For the case when the fourth-degree polynomial trajectory is used, the values of the initial and final joint angles are as follows

Link [deg]	θ_1	θ_2	θ_3	θ_4	θ_5	θ_6
Start	20	10	10	10	20	10
Stop	50	90	120	80	60	100

Table 2 The initial and final values of the joints

When determining the trajectory, based on the kinematic model of the ABB7600 robot, two simulation scenarios are taken into consideration. The first scenario assumes that both initial and final angular velocities, as well as angular accelerations, are zero, while the second scenario considers an initial angular velocity of 1.5 degrees/s. Simulations for the two cases described above were conducted using the Matlab simulation environment.

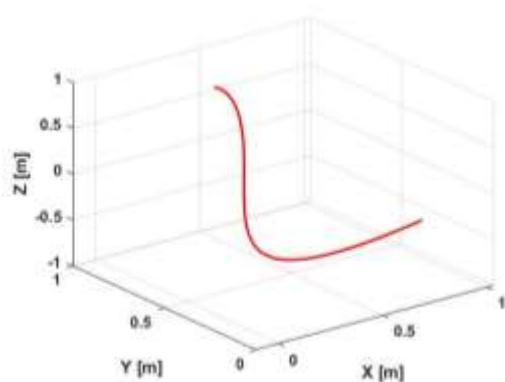


Figure 3.4 End effector trajectory case 1

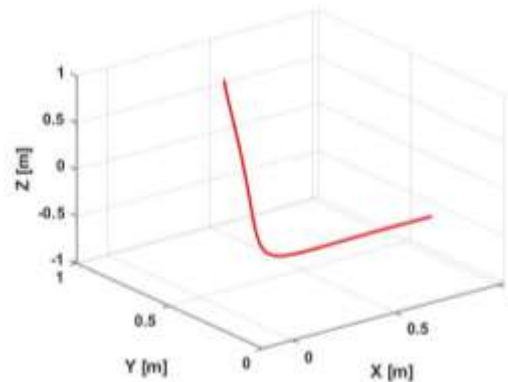


Figure 3.5 End effector trajectory case 2

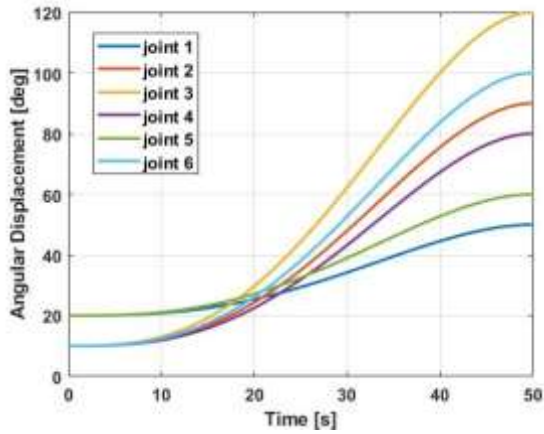


Figure 3.6 Angular displacement case 1

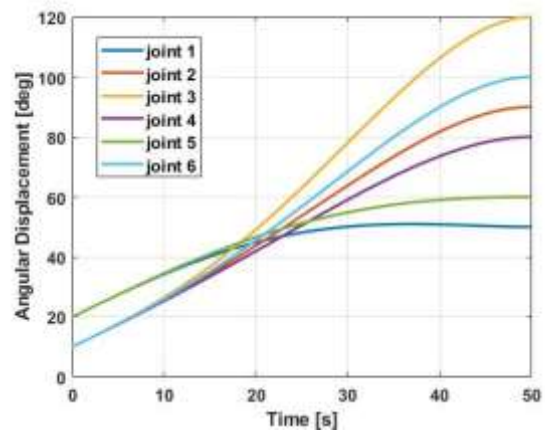


Figure 3.7 Angular displacement case 2

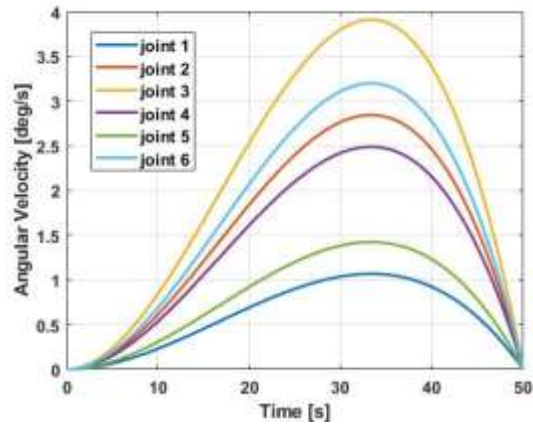


Figure 3.8 Angular velocity case 1

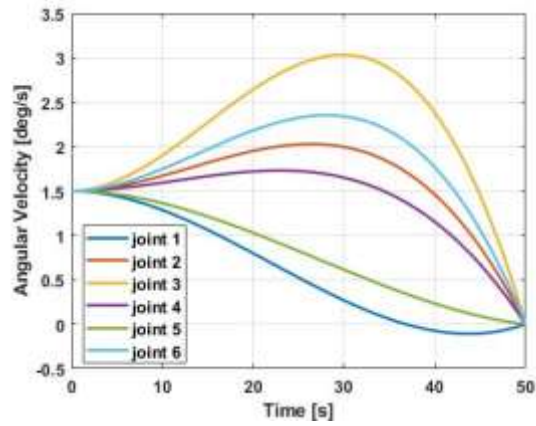


Figure 3.9 Angular velocity case 2

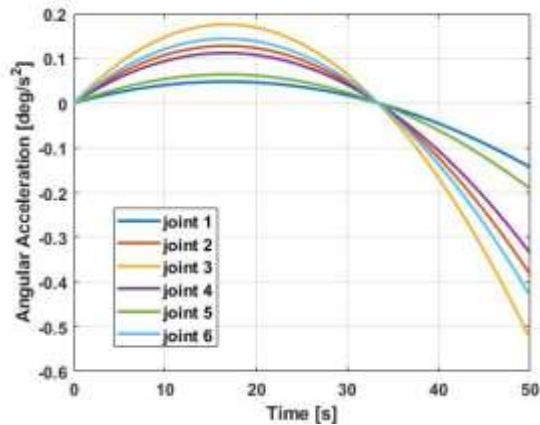


Figure 3.10 Angular acceleration case 1

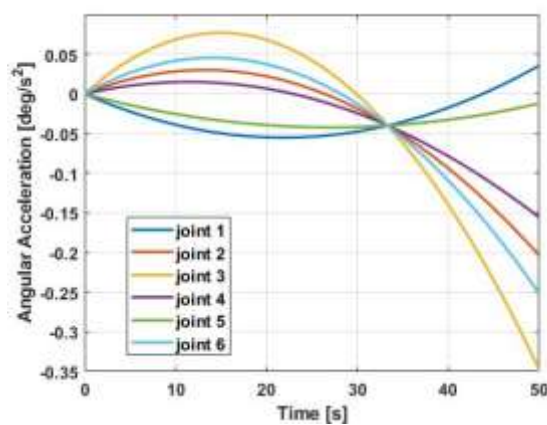


Figure 3.11 Angular acceleration case 2

As observed in Fig. 3.4 and Fig. 3.5, there are significant differences in the obtained end-effector trajectories, these being significant due to the modification of the initial velocity value. It is important to note that the simulation time was fixed at 50s for both cases. Due to the variations in velocity and acceleration between the two trajectories, energy consumption and the demand on the robot's motors may vary, as the aim is to reach the final position. A trajectory with zero initial and final acceleration will impose lower demands on the motors,

whereas a trajectory with an imposed initial velocity may push the motors to their maximum capacity.

Since the goal is to achieve smooth and shock-free motion, choosing the quartic interpolation method minimizes acceleration variation. This study lays the theoretical foundations for an experimental simulation to verify the validity of the obtained results and ensure they remain within acceptable limits. The experimental analysis, which will serve as an analysis for landing at a fixed point on a mobile platform, will be conducted at the SpaceSysLab Maneciu Laboratory of the National Institute for Aerospace Research "Elie Carafoli.

3.7. Conclusions

This chapter presents the development of the kinematic and dynamic model of a six-degree-of-freedom serial manipulator, for the presented simulations using both the Matlab and RobotStudio environments. The solution obtained in the case of the study of the direct kinematics of the robot was based on the use of Denavit-Hartenberg parameters, and the one in the case of the inverse kinematics used an iterative calculation procedure. Of interest was obtaining a mathematical model in terms of inverse kinematics for a serial manipulator with six degrees of freedom, the procedure used taking into account all the constraints on the variables, as well as the analytical determination of the Jacobian.

Further developments aim to enhance the control of the end effector of the serial manipulator operating with flexible elements, which relies on the kinematic and dynamic model presented within this chapter. Additionally, a trajectory of the end effector of the ABB7600 robot has been generated, and the variation of its six joint angles, as well as angular velocities and angular accelerations, has been monitored based on certain input parameters.

Chapter 4

Dynamic modeling of a parallel manipulator

A general Gough-Stewart platform is a parallel manipulator with six prismatic actuators, typically hydraulic jacks or linear electric actuators, which are attached in pairs in three positions on the platform base over three points mounted on a superior platform. The platform has six degrees of freedom, and the direct kinematics problem involves determining the position (position and orientation) of the moving platform relative to the base, given the length of the legs and the coordinates of the attachment points in its local reference frame. [2]

4.1. Kinematic analysis of the Stewart platform

Inverse kinematics determines the lengths of the actuators based on the position and orientation of the Stewart platform. The inverse kinematics model is developed based on simplified models, as found in works [25], [32], [38]. Also, inverse kinematics deals with the mathematical problem of describing the position and orientation of the platform in terms of actuator variables.

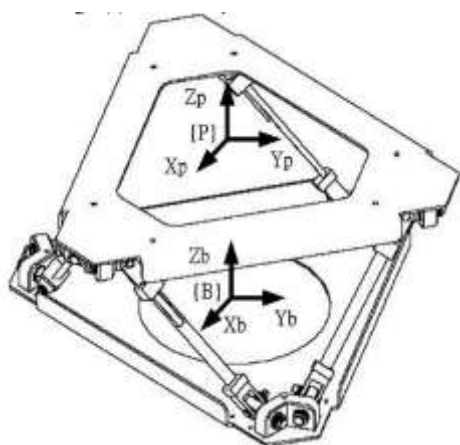


Figure 4.1 Coordinate frames Stewart platform [48]

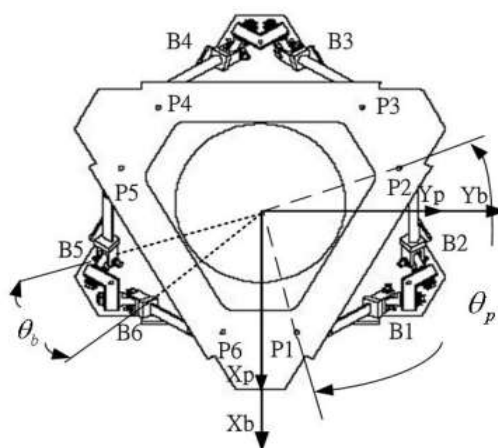


Figure 4.2 Positioning of points on the Stewart platform [48]

By adopting appropriate coordinate transformations and determining the points on the lower and upper platform, the actuation vector L_i corresponding to each actuator can be derived

$$\{L_i\} = [R] \cdot \{P_i\} + \{P\} - \{B_i\}, i = 1,2,3 \dots 6 \quad (4.1)$$

where the vector $\{P\} = \begin{Bmatrix} x \\ y \\ z \end{Bmatrix}$ represents the position of the coordinate system $\{P\}$.

Given that the length of the actuator is $l_i = |L_i|$, an inverse kinematics solution is obtained

$$\{L_i\} = \begin{Bmatrix} r_{11} \cdot P_{ix} + r_{12} \cdot P_{iy} + x - B_{ix} \\ r_{21} \cdot P_{ix} + r_{22} \cdot P_{iy} + y - B_{iy} \\ r_{31} \cdot P_{ix} + r_{32} \cdot P_{iy} + z \end{Bmatrix} \quad (4.2)$$

$$l_i = |L_i| = \sqrt{(r_{11} \cdot P_{ix} + r_{12} \cdot P_{iy} + x - B_{ix})^2 + (r_{21} \cdot P_{ix} + r_{22} \cdot P_{iy} + y - B_{iy})^2 + (r_{31} \cdot P_{ix} + r_{32} \cdot P_{iy} + z)^2} \quad (4.3)$$

$$l_i^2 = x^2 + y^2 + z^2 + r_p^2 + r_B^2 + 2(r_{11}P_{ix} + r_{12}P_{iy})(x - B_{ix}) + 2(r_{21}P_{ix} + r_{22}P_{iy})(y - B_{iy}) + 2(r_{31}P_{ix} + r_{32}P_{iy})z - 2(xB_{ix} + yB_{iy}) \quad (4.4)$$

The ***direct kinematics*** of the upper platform of the six-degree-of-freedom parallel manipulator plays an important role in controlling or visualizing the motion of the platform, but it is difficult to define due to the nonlinearity and complexity of the platform. A popular method for solving the derivative problem is the Newton Raphson method, but it suffers from repetitive steps before the solution converges and therefore cannot become a real-time solution. Also, by imposing wrong values of the initial conditions this method can lead to an infinite loop in the solution. However, the general expression can be expressed

$$f(x, y, z, \alpha, \beta, \gamma) = x^2 + y^2 + z^2 + r_p^2 + r_B^2 + 2(r_{11}P_{ix} + r_{12}P_{iy})(x - B_{ix}) + 2(r_{21}P_{ix} + r_{22}P_{iy})(y - B_{iy}) + 2(r_{31}P_{ix} + r_{32}P_{iy})z - 2(xB_{ix} + yB_{iy}) - l_i^2 \quad (4.5)$$

4.2. The dynamic equations of the Stewart platform

The dynamic analysis of the parallel manipulator is much more difficult compared to that of the serial manipulator due to the existence of multiple kinematic chains, all connected by the mobile platform. So, in this subchapter, the Lagrange formulation will be used, because it offers a much better structure to describe the dynamics of the manipulator. Regarding the derivation of the dynamic equations of the Stewart platform, the whole system will be separated into two parts, the mobile platform and the actuators. Also, the kinetic and potential energies will be calculated for both sides. Consequently, the dynamic equations will be derived using these energies.

4.2.1. Dynamic analysis of actuators

Each Stewart platform actuator is composed of two parts: the moving part (piston) and the fixed part (cylinder), as seen in the figure below. The movable component is connected to the upper platform by a ball joint, while the fixed component is connected to the base platform by a Hooke joint.

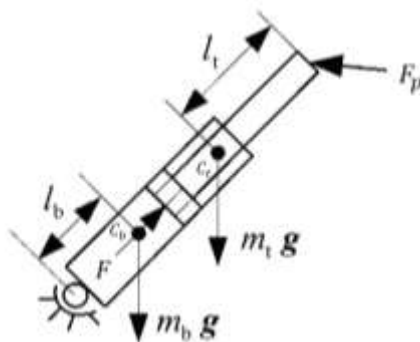


Figure 4.3 Stewart platform actuator

As can be seen in Figure 4.3, the centers of gravity are defined for each individual component, respectively the distances from the two joints to the centers of gravity. Also, for the calculation of the position and orientation of the actuators, the figure below will be taken into account, where the coordinate systems of the center of the base $B(x_B, y_B, z_B)$, respectively of one of the joints of the points of the lower platform, $B_i(x_{B_i}, y_{B_i}, z_{B_i})$.

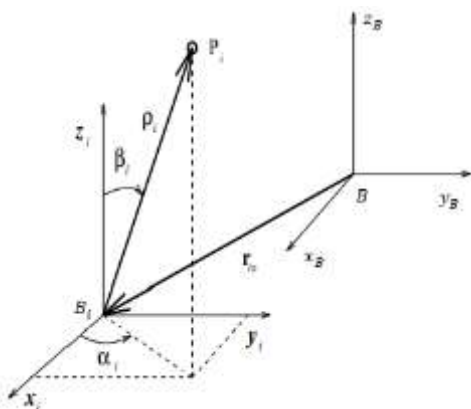


Figure 4.4 $\vec{B_i P_i}$ in spherical coordinates

As observed in Figure 4.4, the position vector of point P_i can also be defined using spherical coordinates, where

$$\begin{Bmatrix} x_P \\ y_P \\ z_P \end{Bmatrix} = \{r_{i_0}\} + \{\rho_i\}, \quad i = \overline{1,6} \quad (4.6)$$

with

- $\{r_{i_0}\} = \begin{Bmatrix} x_{i_0} \\ y_{i_0} \\ z_{i_0} \end{Bmatrix}$ representing the vector $\vec{B B_i}$
- $\{\rho_i\} = \begin{Bmatrix} \rho_i \cos \alpha_i \sin \beta_i \\ \rho_i \sin \alpha_i \sin \beta_i \\ \rho_i \cos \beta_i \end{Bmatrix}$ representing the vector $\vec{B_i P_i}$ expressed in spherical coordinates.

Regarding the calculation of linear and angular velocities of all the links, these will be derived using the independent Cartesian velocities of the platform $[\dot{x} \ \dot{y} \ \dot{z} \ \dot{\omega}_x \ \dot{\omega}_y \ \dot{\omega}_z]$.

Once the position vector of point P_i has been determined, the velocity of the link can also be determined accordingly

$$\{\lambda_i\} = [C_i^{-1}] \begin{Bmatrix} \dot{x}_P \\ \dot{y}_P \\ \dot{z}_P \end{Bmatrix} \quad (4.7)$$

The linear and angular accelerations of the links are determined based on the Cartesian accelerations of the platform $[\ddot{x} \ \ddot{y} \ \ddot{z} \ \ddot{\omega}_x \ \ddot{\omega}_y \ \ddot{\omega}_z]$, obtaining

$$\begin{Bmatrix} \ddot{x}_P \\ \ddot{y}_P \\ \ddot{z}_P \end{Bmatrix} = \{\ddot{\rho}_{i_r}\} + \{\dot{\omega}_i\} \times \{\rho_i\} + \{\omega_i\} \times (\{\dot{\rho}_{i_r}\} + \{\omega_i\} \times \{\rho_i\}), \quad i = \overline{1,6} \quad (4.8)$$

where

$$\{\ddot{\rho}_{i_r}\} = \begin{Bmatrix} \ddot{\rho}_i \cos \alpha_i \sin \beta_i \\ \ddot{\rho}_i \sin \alpha_i \sin \beta_i \\ \ddot{\rho}_i \cos \beta_i \end{Bmatrix} \quad (4.9)$$

$$\{\dot{\omega}_i\} = \begin{Bmatrix} -\ddot{\beta}_i \sin \alpha_i - \dot{\beta}_i \dot{\alpha}_i \cos \alpha_i \\ \ddot{\beta}_i \cos \alpha_i - \dot{\beta}_i \dot{\alpha}_i \sin \alpha_i \\ \ddot{\alpha}_i \end{Bmatrix} \quad (4.10)$$

Given that $\{\lambda_i\} = \begin{Bmatrix} \ddot{\rho}_i \\ \ddot{\alpha}_i \\ \ddot{\beta}_i \end{Bmatrix}$ it has been obtained

$$\{\mathbf{h}_i\} = \begin{Bmatrix} \ddot{x}_P - 2\dot{\rho}_i \dot{\beta}_i c_{\alpha_i} c_{\beta_i} + 2\dot{\rho}_i \dot{\alpha}_i s_{\alpha_i} s_{\beta_i} + 2\rho_i \dot{\alpha}_i \dot{\beta}_i s_{\alpha_i} c_{\beta_i} + \rho_i \dot{\alpha}_i^2 c_{\alpha_i} s_{\beta_i} + \rho_i \dot{\beta}_i^2 c_{\alpha_i} s_{\beta_i} \\ \ddot{y}_P - 2\dot{\rho}_i \dot{\beta}_i s_{\alpha_i} c_{\beta_i} - 2\dot{\rho}_i \dot{\alpha}_i c_{\alpha_i} s_{\beta_i} - 2\rho_i \dot{\alpha}_i \dot{\beta}_i c_{\alpha_i} c_{\beta_i} + \rho_i \dot{\alpha}_i^2 s_{\alpha_i} s_{\beta_i} + \rho_i \dot{\beta}_i^2 s_{\alpha_i} s_{\beta_i} \\ \ddot{z}_P + c_{\beta_i} + 2\dot{\rho}_i \dot{\beta}_i s_{\beta_i} + \rho_i \dot{\beta}_i^2 c_{\beta_i} \end{Bmatrix} \quad (4.11)$$

where the notations have been made $c_{\alpha_i} = \cos \alpha_i$, $c_{\beta_i} = \cos \beta_i$, $s_{\alpha_i} = \sin \alpha_i$, $s_{\beta_i} = \sin \beta_i$.

4.2.2. Dynamic analysis of the Stewart platform

The dynamic analysis of the Stewart platform can be performed by applying the Lagrange equations [60], [70]

$$\frac{d}{dt} \left(\frac{\partial E}{\partial \dot{q}_k} \right) - \frac{\partial E}{\partial q_k} + \frac{\partial U}{\partial q_k} = Q_k \quad (4.12)$$

In this case q_k represents the generalized coordinates, respectively $q_k = [x \ y \ z \ \varphi \ \theta \ \psi]^T$, Q_k represents the generalized forces, E and U represent the kinetic energy and potential energy of the upper platform, respectively.

The translational kinetic energy resulting from the translational motion of the center of mass is defined as follows

$$E_t = \frac{1}{2} m_p (\dot{p}_x^2 + \dot{p}_y^2 + \dot{p}_z^2) \quad (4.13)$$

where m_p is the mass of the upper platform, \dot{p}_x^2 , \dot{p}_y^2 , \dot{p}_z^2 are the velocities along the three axes of the center of mass.

Regarding the rotational motion of the mobile platform around its center of mass, the rotational kinetic energy can be expressed as follows

$$E_r = \frac{1}{2} \omega_p^T I_p \omega_p \quad (4.14)$$

where I_p and ω_p are the moment of inertia of rotation and the angular velocity of the mobile platform.

The total kinetic energy of the upper platform, expressed in a compact form, is given by

$$E = E_t + E_c = \frac{1}{2} [\dot{P}_x \ \dot{P}_y \ \dot{P}_z \ \dot{\phi} \ \dot{\theta} \ \dot{\psi}] [M] \begin{Bmatrix} \dot{P}_x \\ \dot{P}_y \\ \dot{P}_z \\ \dot{\phi} \\ \dot{\theta} \\ \dot{\psi} \end{Bmatrix} \quad (4.15)$$

where M is a 6x6 diagonal matrix of the upper platform.

Furthermore, the potential energy of the upper platform is given by

$$U = [0 \ 0 \ m_p g \ 0 \ 0 \ 0] \begin{Bmatrix} P_x \\ P_y \\ P_z \\ \phi \\ \theta \\ \psi \end{Bmatrix} = m_p g P_z \quad (4.16)$$

where g represents the gravitational acceleration.

The formulation of the equation using redundant coordinates (equations that use more coordinates than degrees of freedom of the underlying system) of the mechanism's kinematics is as follows

$$M(X)\ddot{X} + C(X, \dot{X})\dot{X} + G(X) = J^T(X)\tau \quad (4.17)$$

where $M(X)$ is the mass matrix, $C(X)$ is the term for the Coriolis and centrifugal forces, $G(X)$ is the gravitational force, J is the Jacobian matrix.

The Coriolis force matrix, $C(q, \dot{q})$, is defined as follows

$$C(q, \dot{q}) = \frac{1}{2} \{M(\dot{q}) + U_M^T - U_M\} \quad (4.18)$$

where U_M is determined using the Kronecker product.

4.3. Case study

In this section, several dynamic simulations were performed to highlight the inertia effect of the actuators and their components on the dynamics of the entire system. Eight simulation cases were considered, one of which represented a sinusoidal trajectory along the z-axis while keeping the platform's orientation constant during motion.

$[\varphi, \theta, \psi]^T = [0, 0, 0]^T$	
$\begin{bmatrix} x \\ y \\ z \end{bmatrix}$	$= \begin{bmatrix} -0.2 \\ -0.3 \\ -0.08 * \cos(\omega * t) \end{bmatrix}$

Table 3 Predefined sinusoidal trajectory simulation case

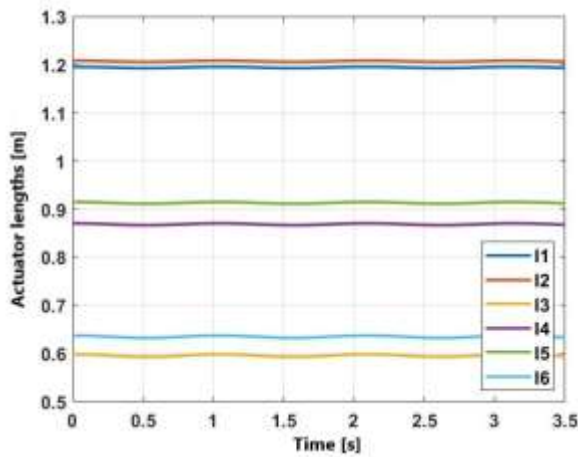


Figure 4.5 Actuator lengths as a function of time

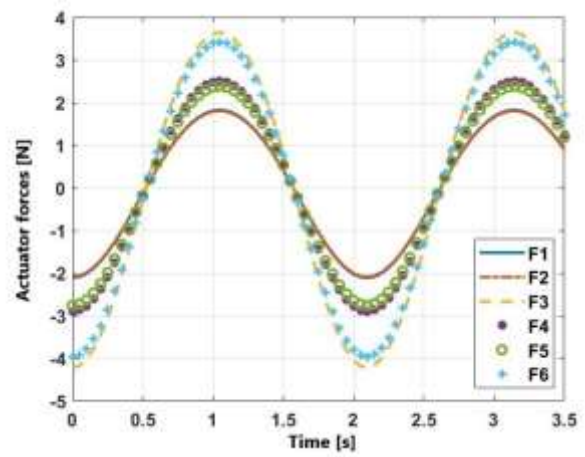


Figure 4.6 Actuator forces as a function of time

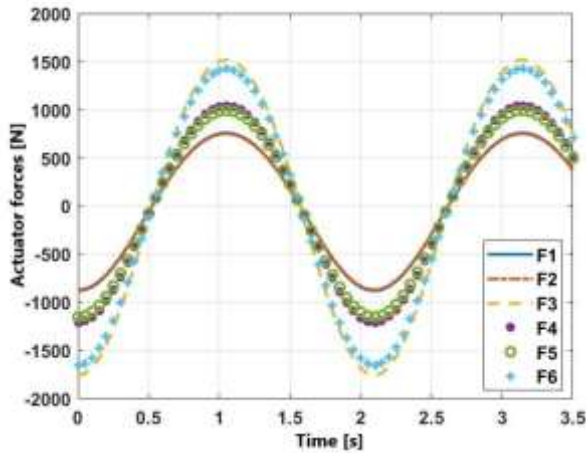


Figure 4.7 Actuator forces as a function of time with a payload of 1250kg

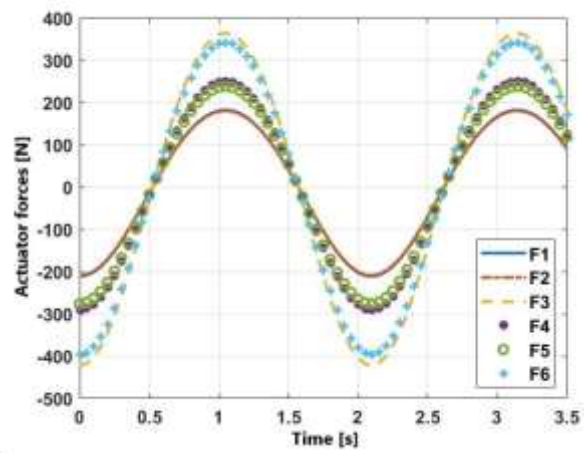


Figure 4.8 Actuator forces as a function of time with a payload of 300kg

Sensitivity analysis was also conducted, which is a method used to examine how changes in parameters or input variables influence the outcome or effectiveness of a system. The sensitivity analysis procedure involves identifying the key parameters for the performance of the Stewart platform, those parameters expected to exert the most significant

influence on the system. Subsequently, a systematic alteration of certain parameters while keeping others constant is considered, leading to three simulations in this case.

In the initial phase, the input parameters of the Stewart platform were kept the same as in the sixth simulation case. Later, only the angle θ was modified, and in the last simulation, the angle φ was altered.

The specific parameters for the sixth simulation case are as follows

$[\varphi, \theta, \psi]^T = [0, 0, 20]^T$
$\begin{bmatrix} x \\ y \\ z \end{bmatrix} = \begin{bmatrix} -0.3 + 0.25 * \sin(\omega * t) \\ -0.4 * \sin(\omega * t) \\ 0.7 + 0.5 * \sin(\omega * t) \end{bmatrix}$

Table 4 Simulation case – change in ψ angle

In the figures below, variations in forces have been identified based on changes in input parameters.

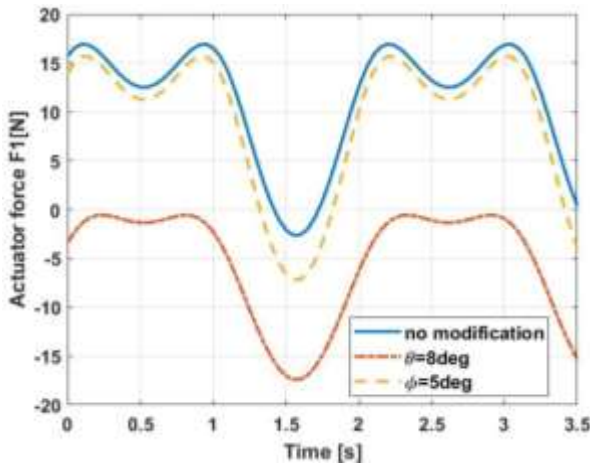


Figure 4.9 Sensitivity analysis for F1

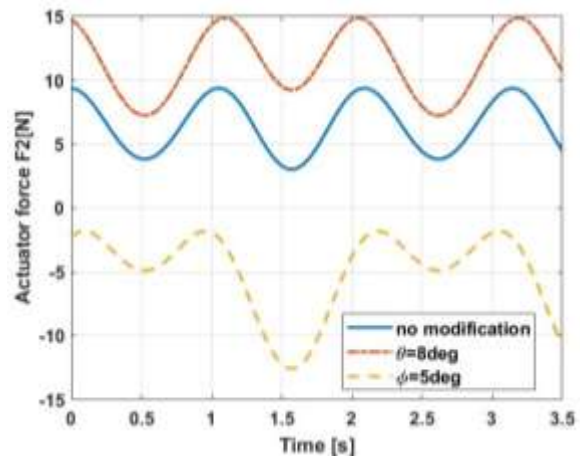


Figure 4.10 Sensitivity analysis for F2

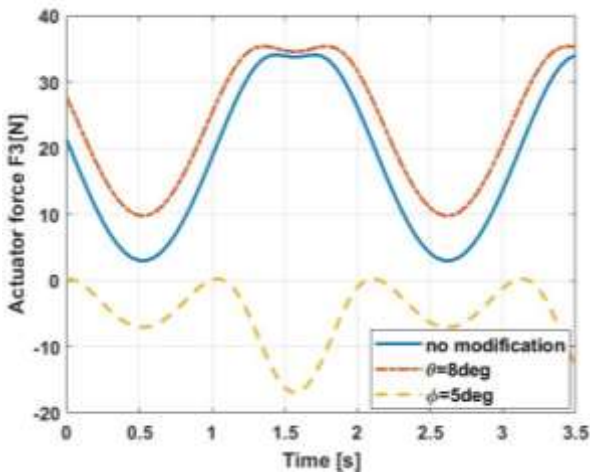


Figure 4.11 Sensitivity analysis for F3

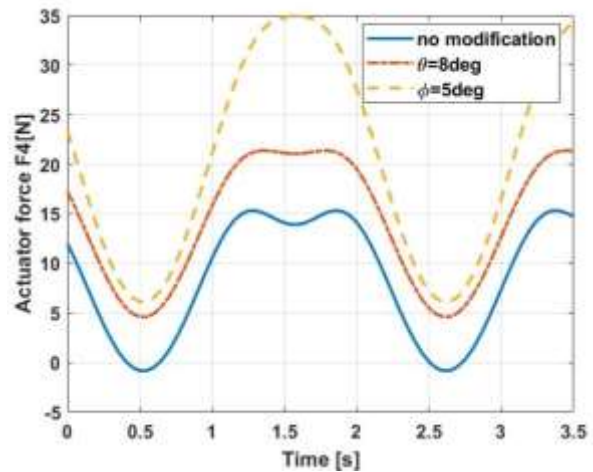


Figure 4.12 Sensitivity analysis for F4

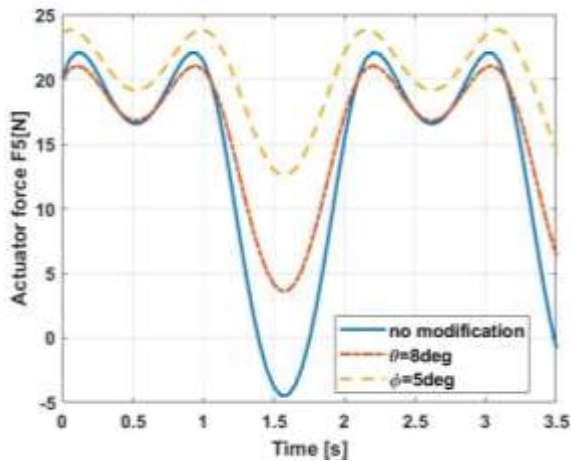


Figure 4.13 Sensitivity analysis for F5

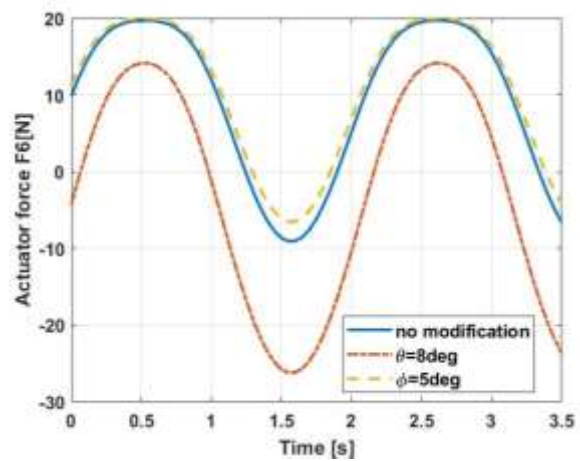


Figure 4.14 Sensitivity analysis for F6

4.4. Conclusions

In this chapter, the closed-form dynamic equations of a parallel manipulator were presented using the Lagrangian formalism. The configuration considered was a Stewart platform with six degrees of freedom.

The algorithm was implemented using the Matlab simulation environment, and the numerical results were analyzed to validate the presented dynamic formulation. The simulation results demonstrate the feasibility of deriving explicit dynamic equations in the task space for a six-degree-of-freedom manipulator, thereby obtaining the actuation forces on the mobile platform's actuators. The preceding case studies defined predefined motions of the mobile platform along a single axis (x , y , z) or based on the attitude angles (φ , θ , ψ). The variations in actuator forces and their motion during the simulations were examined. Overall, the presented studies provide insights into the imposed motion of the mobile platform and the resulting actuator forces. This analysis contributes to a better understanding of the dynamic behavior of the parallel manipulator system and its performance under different motion scenarios.

Chapter 5

Landing of an aerial vehicle on a mobile platform

In the specialized literature, there is an increasing interest in autonomous vertical takeoff and landing (VTOL) aerial vehicles for various applications, including aerial imaging and surveillance. An important function of such aerial vehicles is autonomous landing on fixed or mobile platforms, which is often challenging due to strict safety constraints, collision avoidance, requirements for gentle contact, and limited landing time. Therefore, an appropriate landing trajectory can minimize the total landing time, and generating it in real-time prior to the landing maneuver is crucial to meet safety constraints [72].

The objective of this chapter is to determine different landing trajectories for a spacecraft positioned at the final end of a six-degree-of-freedom serial manipulator, specifically at its end effector, on a six-degree-of-freedom Stewart platform. The manipulators used for this purpose are defined in Chapters 3 and 4, and it is known that once the type of motion is defined, the robot is typically optimized for fast cycle times. Therefore, this motion requires an optimal trajectory in time, considering the kinematic constraints.

5.1. Dynamic model of the aerial vehicle

Regarding the autonomous landing of a spacecraft on a moving platform, it is crucial to accurately estimate the position of both the spacecraft and the landing platform. In this work, it is assumed that the spacecraft is a rigid body with a uniform mass distribution, constant mass, and the center of mass coinciding with the geometric center.

The dynamic model of the spacecraft is obtained using the Lagrangian formalism, where an inertial coordinate system and a coordinate system attached to the spacecraft are considered, as shown in the figure below

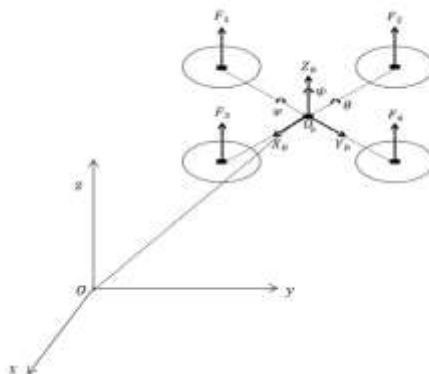


Figure 5.1 Coordinate system of the spacecraft

Figure 5.1 illustrates an inertial reference frame $Oxyz$ and a body reference frame $O_d x_d y_d z_d$. Considering the spacecraft as a rigid body with the center of mass coinciding with the origin of the body reference frame, the state variables of the system were taken into account, including position, linear velocity, angular velocity, and the orientation of the spacecraft.

In this chapter, the Lagrangian formalism was used to determine the state equations, specifically for the spacecraft's dynamics

$$\begin{aligned}
 \frac{d}{dt} \left(\frac{\partial L}{\partial \dot{\varphi}} \right) - \frac{\partial L}{\partial \varphi} &= \tau_{\varphi} \\
 \frac{d}{dt} \left(\frac{\partial L}{\partial \dot{\theta}} \right) - \frac{\partial L}{\partial \theta} &= \tau_{\theta} \\
 \frac{d}{dt} \left(\frac{\partial L}{\partial \dot{\psi}} \right) - \frac{\partial L}{\partial \psi} &= \tau_{\psi}
 \end{aligned} \tag{5.1}$$

where $L = E_c - E_p$, E_c is the kinetic energy, E_p is the potential energy, τ represents the total moments acting around the x, y, z axes.

Considering the mechanical symmetry of the quadrotor, both the moments of inertia and the inertia products are considered negligible. Therefore, the kinetic energy of the quadrotor can be rewritten as follows

$$E_c = \frac{1}{2} I_{xx} (\dot{\varphi} - \dot{\psi} \sin \theta)^2 + \frac{1}{2} I_{yy} (\dot{\theta} \cos \varphi + \dot{\psi} \sin \varphi \cos \theta)^2 + \frac{1}{2} I_{zz} (\dot{\theta} \sin \varphi - \dot{\psi} \cos \varphi \cos \theta)^2 \tag{5.2}$$

The potential energy of the quadrotor is defined as follows

$$E_p = mgr_z = mg(-x \sin \theta + y \cos \theta \sin \varphi + z \cos \theta \cos \varphi) \tag{5.3}$$

Furthermore, the total moments acting on the three axes are defined as follows

$$\begin{aligned}
 \tau_x &= b \cdot l \cdot (\Omega_4^2 - \Omega_2^2) + J_r \omega_y (\Omega_1 + \Omega_3 - \Omega_2 - \Omega_4) \\
 \tau_y &= b \cdot l \cdot (\Omega_3^2 - \Omega_1^2) + J_r \omega_x (-\Omega_1 - \Omega_3 + \Omega_2 + \Omega_4) \\
 \tau_z &= d \cdot (\Omega_1^2 - \Omega_2^2 + \Omega_3^2 - \Omega_4^2)
 \end{aligned} \tag{5.4}$$

To derive the equations of motion for a rigid body under the action of external forces applied to the center of mass and expressed in the body-fixed coordinate system, the Newton-Euler formalism will be used.

The equations of motion for the quadrotor can be derived using Newton's second law of motion, which is expressed in the inertial reference frame. The two vector equations can be exemplified as follows

$$F = \frac{d}{dt} (mV) \tag{5.5}$$

$$M = \frac{d}{dt} (H) \tag{5.6}$$

The thrust forces acting on the quadrotor, expressed in the inertial reference frame, can be written as follows

$$\begin{aligned}
 F_x &= (\sin \varphi \sin \psi + \cos \varphi \sin \theta \cos \psi) U_1 \\
 F_y &= (-\cos \psi \sin \varphi + \sin \psi \sin \theta \cos \varphi) U_1 \\
 F_z &= \cos \psi \cos \varphi U_1
 \end{aligned} \tag{5.7}$$

where $U_1 = \sum_{i=1}^4 T_i = T_1 + T_2 + T_3 + T_4$, representing the sum of the four translational motion forces generated by the propellers on each rotor, and they can be defined as follows $T_i = b \Omega_i^2$, with $i = \overline{1,4}$.

The forces acting on the quadrotor are the thrust forces generated by the propellers, denoted as F_t and the drag forces, denoted as F_r .

By expanding the equations mentioned above, the dynamics of the quadrotor can be obtained

$$\begin{aligned}
 \ddot{x} &= (\sin \varphi \sin \psi + \cos \varphi \sin \theta \cos \psi) \frac{U_1}{m} - \frac{1}{2m} C_D \rho A \dot{x}^2 \\
 \ddot{y} &= (-\cos \psi \sin \varphi + \sin \psi \sin \theta \cos \varphi) \frac{U_1}{m} - \frac{1}{2m} C_D \rho A \dot{y}^2 \\
 \ddot{z} &= \cos \psi \cos \varphi \frac{U_1}{m} - g - \frac{1}{2m} C_D \rho A \dot{z}^2 \\
 \ddot{\varphi} &= \frac{(I_{yy} - I_{zz})}{I_{xx}} \dot{\theta} \dot{\psi} - \frac{J_r \dot{\theta} \Omega_r}{I_{xx}} + \frac{U_2}{I_{xx}} \\
 \ddot{\theta} &= \frac{(I_{zz} - I_{xx})}{I_{yy}} \dot{\varphi} \dot{\psi} + \frac{J_r \dot{\varphi} \Omega_r}{I_{yy}} + \frac{U_3}{I_{yy}} \\
 \ddot{\psi} &= \frac{(I_{xx} - I_{yy})}{I_{zz}} \dot{\varphi} \dot{\theta} + \frac{U_4}{I_{zz}}
 \end{aligned} \tag{5.8}$$

5.2. Landing phase

The dynamic model of the Stewart platform is considered as presented in Chapter 4. Additionally, it is assumed that the platform undergoes motion along the z axis, denoted as z_p , as observed

$$z_p = \sum_{i=1}^4 A_i \sin(\omega_i t) \tag{5.9}$$

where A_i represents the amplitude, ω_i represents the angular velocity.

Using the equations of motion of the model presented in the previous subsection, the expressions for the nonholonomic constraints are extracted as follows

$$\varphi_{desired} = \arcsin \left(\frac{\dot{x} \sin \psi - \dot{y} \cos \psi}{\sqrt{\dot{x}^2 + \dot{y}^2 + (\dot{z} + g)^2}} \right) \tag{5.10}$$

$$\theta_{desired} = \arctg \left(\frac{\dot{x} \cos \psi + \dot{y} \sin \psi}{\dot{z} + g} \right) \tag{5.11}$$

Regarding the landing process, it is assumed that the quadrotor model is positioned above the platform. The landing control is carried out using the Backstepping method, as described in [69]. The state variables used in this landing process are $[\varphi, \dot{\varphi}, \theta, \dot{\theta}, \psi, \dot{\psi}, x, \dot{x}, y, \dot{y}, z, \dot{z}]$ and the control variables are defined as $[U_1, U_2, U_3, U_4]$.

The linearized system obtained

$$\begin{aligned}
 \dot{x}_1 &= x_2 \\
 \dot{x}_2 &= \frac{(I_{yy} - I_{zz})}{I_{xx}} x_4 x_6 + \frac{1}{I_{xx}} U_2 - \frac{J_r \Omega_r}{I_{xx}} x_4 \\
 \dot{x}_3 &= x_4 \\
 \dot{x}_4 &= \frac{I_{zz} - I_{xx}}{I_{yy}} x_2 x_6 + \frac{1}{I_{yy}} U_3 - \frac{J_r \Omega_r}{I_{yy}} x_2 \\
 \dot{x}_5 &= x_6 \\
 \dot{x}_6 &= \frac{I_{xx} - I_{yy}}{I_{zz}} x_2 x_4 + \frac{1}{I_{zz}} U_4 \\
 \dot{x}_7 &= x_8 \\
 \dot{x}_8 &= \frac{1}{m} U_1 [\cos(x_1) \sin(x_3) \cos(x_5) + \sin(x_1) \sin(x_5)] \\
 \dot{x}_9 &= x_{10} \\
 \dot{x}_{10} &= \frac{1}{m} U_1 [\cos(x_1) \sin(x_3) \sin(x_5) - \sin(x_1) \cos(x_5)]
 \end{aligned} \tag{5.12}$$

$$\begin{aligned} \dot{x}_{11} &= x_{12} \\ \dot{x}_{12} &= -g + \frac{1}{m}U_1 \cos(x_1) \cos(x_3) \end{aligned}$$

Two case studies were further considered, the first involving a smooth motion of the mobile platform, while the second involved a rapid motion of the mobile platform according to equation (5.9). The input parameters considered were $m_{quad} = 40kg$; $x_{quad} = x_{platf} = 12 m$; $y_{quad} = y_{platf} = 7 m$; $z_{quad} = 10 m$; $\varphi_{quad} = 3^\circ$, $\theta_{quad} = 8^\circ$, $\psi_{quad} = 5^\circ$.

- Case I

$$A_1 = 0.2 ; A_2 = 0.6 ; A_3 = 0.5 ; A_4 = 0.3 ; \omega_1 = \frac{3\pi}{10} ; \omega_2 = \frac{2\pi}{5} ; \omega_3 = \frac{\pi}{5} ; \omega_4 = \frac{\pi}{4}$$

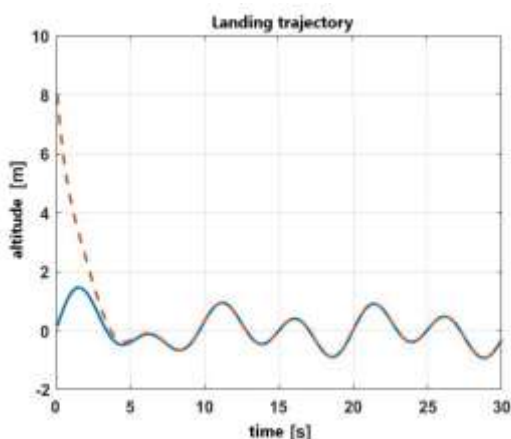


Figure 5.2 Quadcopter trajectory case I

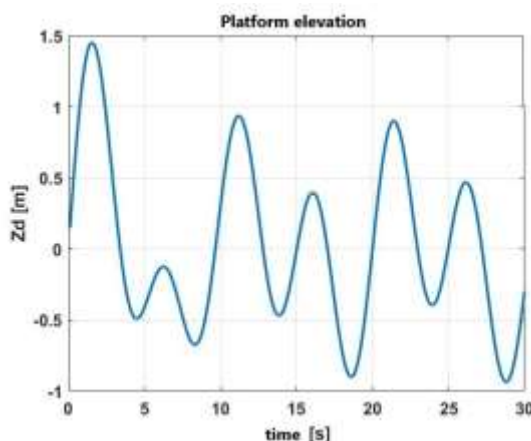


Figure 5.3 Platform elevation case I

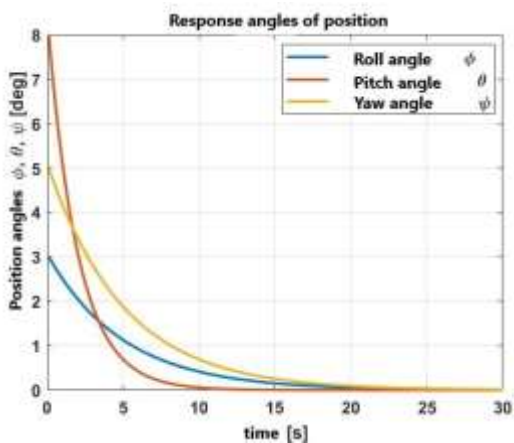


Figure 5.4 Quadcopter attitude angles case I

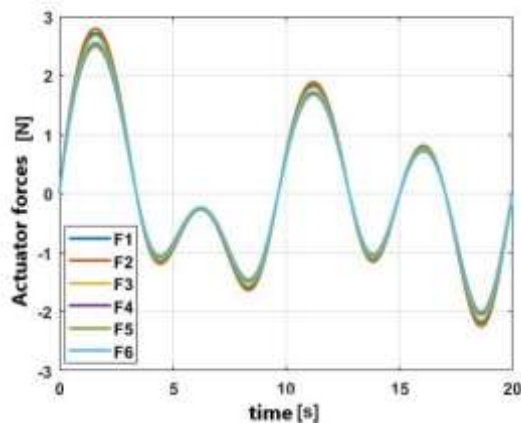


Figure 5.5 Variation of actuator forces case I

- Case II

$$\omega_1 = \frac{6\pi}{5} ; \omega_2 = \pi ; \omega_3 = \frac{\pi}{2} ; \omega_4 = \frac{3\pi}{4}$$

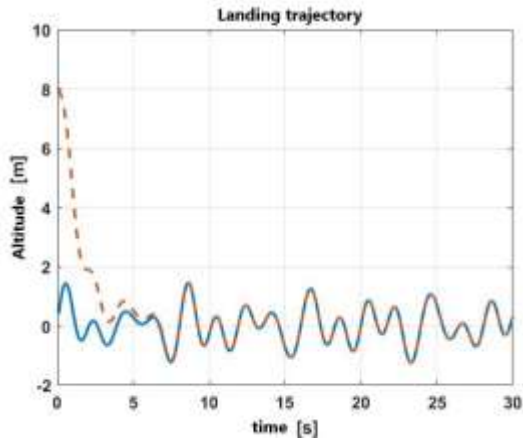


Figure 5.6 Quadcopter trajectory case II

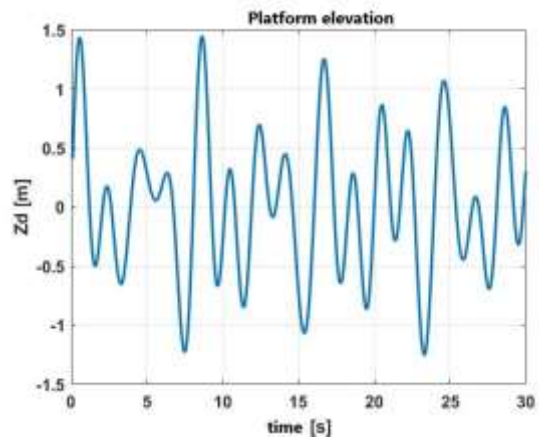


Figure 5.7 Platform elevation case II

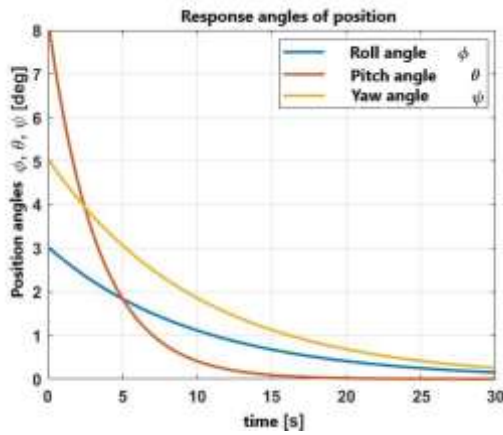


Figure 5.8 Quadcopter attitude angles case II

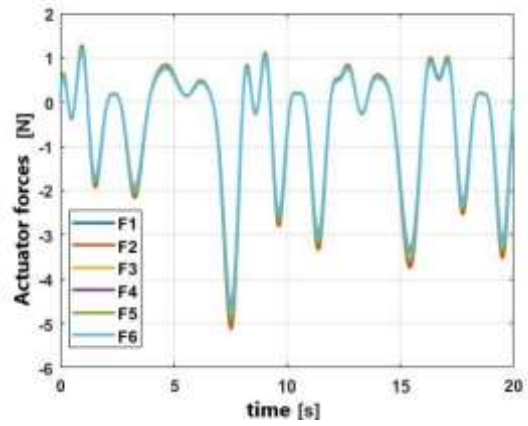


Figure 5.9 Variation of actuator forces case II

5.3. Conclusions

This chapter presents the simulation of two vertical landing cases of a quadcopter on a Stewart platform. As observed from the experimental diagrams, the introduced backstepping controller demonstrates a high capability of controlling the position angles in the presence of various disturbances. The aim of this chapter is to showcase the relative motion of the vehicle with respect to the mobile platform, each model having six degrees of freedom. As seen in the previously presented figures, as the platform elevation becomes more dynamic, the control of the quadcopter in terms of attitude becomes more challenging, taking a longer time to stabilize.

In this study, the vertical landing phase of an aerial vehicle on a Stewart platform was proposed, and the dynamic model of the relative motion between the two was derived considering model uncertainties and the landing site effect.

The results of this theoretical analysis and the presented simulations can serve as the basis for further developments focusing on control design and performance analysis of a quadcopter performing dynamic transition processes from autonomous approach to autonomous landing on mobile platforms.

Chapter 6

Experimental analysis

Testing and validation in the preliminary stages of aerial vehicle landing operations are essential to ensure optimal performance of drones in fully automated missions. The development of a new experimental facility aimed to expand the spectrum of possible missions, and the analysis and control of the ABB7600-500 robot's motion involves assessing its capabilities and performance on a rail system over 22 meters long. This was accomplished within the INCAS SpaceSysLab, where a Stewart-type platform was integrated to control the robot's motion in accordance with user-defined automated intentions.

The study of control algorithms for autonomous approach and landing of aerial platforms on mobile/marine platforms involves developing a mathematical model of the vehicle and autonomously controlling the landing using a camera system. The implementation and programming of control algorithms for the marine platform, accounting for atmospheric and marine environment disturbances, is based on a dynamic model with four degrees of freedom.

Vertical landing technology on fixed or mobile platforms represents a significant advancement in the performance of approach and docking missions for aerial vehicles. The control system plays a central role in landing on a mobile platform, eliminating the need for special landing spaces. Additionally, IMU (Inertial Measurement Unit) and laser altimeter sensors are essential for ensuring precise landing. The IMU sensor provides accurate data on position, orientation, and velocity, while the laser altimeter offers precise warnings about proximity to the ground. The integration of these technologies contributes to improving the efficiency and precision of landing.

Experimental analysis involved testing the system in a controlled environment, identifying challenges and risks, and adjusting algorithms for stable and accurate landing. This integrated approach of theory, simulation, and experimentation has contributed to the development of landing technology on mobile platforms, enhancing the efficiency and reliability of unmanned aerial vehicle operations.

Future developments could include algorithm enhancements for landing under complex conditions, the use of advanced sensors, as well as the capability for autonomous landing on unprepared surfaces or in varied environments. Integration with GPS systems could enable precise and autonomous landings in specific locations.

Chapter 7

Rendezvous & docking missions

The technology of rendezvous and docking refers to typical space maneuvers between two vehicles, defined as three phases of movements. The first part of this flight scenario, called "phasing," is performed after launch and is designed to reduce the phase angle in the orbital plane and the altitude difference between the tracking satellite and the target. Once the tracker has captured the target and is positioned behind it, usually at a lower altitude and behind it by tens of kilometers, the first contact between the two satellites can be established, and their relative position can be determined. This phase is called "homing," followed by the closing phase, which aims to bring the tracker within a range of tens to hundreds of meters (depending on the mission). The final stage represents the docking itself, during which the relative state between the docking ports of the target and the tracker is usually crucial. Achieving the necessary control precision for a successful docking mission between two cooperating spacecraft requires a robust and efficient navigation solution.

Orbital mechanics, as described earlier, is based on the mechanics of celestial bodies, and the study of satellites requires fundamental principles. In this regard, Kepler provided three basic empirical laws that describe motion on unperturbed orbits.

Furthermore, in the field of orbital mechanics, the motion of particles through Euclidean space is considered, necessitating the definition of a reference framework, known as a reference system, in which the motion between the tracker and the target is tracked. The two types of reference systems are the inertial system and the non-inertial system, with subsequent subchapters exploring various corresponding motions in these reference systems.

7.1. Trajectories in an inertial reference frame

The inertial reference frame is the one that moves with a constant velocity, without any acceleration or rotation. Considering this, any object moving in an inertial reference frame will obey Newton's first law, meaning it will maintain its state of rest or uniform rectilinear motion, as long as no external forces act upon it.

For a non-holonomic system, the Lagrange equations corresponding to a system with h generalized coordinates are defined as follows

$$\frac{d}{dt} \left(\frac{\partial E}{\partial \dot{q}_k} \right) - \frac{\partial E}{\partial q_k} = Q_k + \sum_{i=1}^n \lambda_i a_{i_k}, \quad k = \overline{1, h} \quad (7.1)$$

These equations are supplemented with certain constraints

$$\sum_{i=1}^n a_{i_k} \dot{q}_k + b_i = 0, \quad i = \overline{1, p} \quad (7.2)$$

The Lagrangian formalism in the inertial reference frame is rewritten as follows

$$\frac{d}{dt} \left(\frac{\partial E}{\partial \dot{q}_k} \right) - \frac{\partial E}{\partial q_k} = Q_k + \frac{\partial U_\Phi}{\partial q_k}, \quad k = \overline{1, h} \quad (7.3)$$

where the function has been denoted as $U_\Phi = \sum_{i=1}^p \lambda_i \Phi_i$.

7.2. Trajectories in noninertial reference frame

When it comes to the mechanics of a non-inertial reference frame, it is a generalization of Newton's laws to any reference frame. Therefore, in this chapter, we will present the Lagrange relations in this reference frame.

The motion of a system of point masses located in the reference frame (T) is characterized by the generalized coordinates $q_1, \dots, q_k, \dots, q_h$.

In the case where the kinetic energy, as well as the velocities, do not depend on the generalized velocities and generalized coordinates, the Lagrange equations can be written with respect to the moving reference frame as follows

$$\frac{d}{dt} \left(\frac{\partial E_e}{\partial \dot{q}_k} \right) - \frac{\partial E_e}{\partial q_k} = Q_k, \quad k = \overline{1, h} \quad (7.4)$$

The transport energy is defined

$$E_t = \frac{1}{2} m \bar{v}_0^2 \left[1 + \sum_{i=1}^n \frac{m_i}{m} \left(\frac{v_{iC}}{v_0} \right)^2 + 2 \frac{\bar{v}_0 \bar{v}_{C_C}}{v_0^2} \right] \quad (7.5)$$

If $\frac{v_{iC}}{v_0} \ll 1$ and $\frac{v_{C_C}}{v_0} \ll 1$ the transport energy can be expressed in terms of the energy with respect to the origin

$$E_t \approx \frac{1}{2} m \bar{v}_0^2 \quad (7.6)$$

Using this approximation, the Lagrange equations can be written in the following form, with the equivalent energy $E_e = E_r + \bar{v}_0 \bar{H}_r + \bar{\omega}_0 \bar{K}_{O_r}$, calculated with respect to a moving reference frame. Assuming that \bar{v}_0 and $\bar{\omega}_0$ do not depend on \dot{q}_k and q_k , the generalized forces Q_k can be calculated with respect to the moving reference frame through virtual work.

In this subsection, the equations of motion resulting from the motion of a non-inertial reference frame with respect to another inertial reference frame are described, according to [33]. Considering the two coordinate systems, a non-inertial reference frame $Oxyz$ coincides with the inertial coordinate system $O_1x_1y_1z_1$ during the motion.

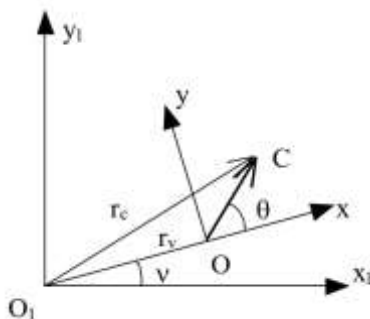


Figure 7.1 Coordinate system

As exemplified in the referenced paper [33], to obtain the equations of motion, specific mathematical analysis equations are used, such as the Lagrange equations. The Lagrange system of equations is described in the previous subsection. Therefore, a first step in

determining the equations of motion is defining the coordinates of the center of mass C in the inertial reference frame, in this case using polar coordinates r_v, v for the inertial reference frame and cylindrical coordinates ρ, θ, z for the moving reference frame. The second step is determining the velocity, for which the notation $\Phi = \dot{r}_v \cos \theta + r_v \dot{v} \sin \theta$ has been used to simplify the calculation, resulting in

$$v^2 = \dot{r}_v^2 + r_v^2 \dot{v}^2 + \dot{\rho}^2 + \rho^2 (\dot{\theta} + \dot{v})^2 + \dot{z}^2 + 2\dot{\rho}\Phi + 2\rho(\dot{\theta} + \dot{v})\frac{\partial\Phi}{\partial\theta} \quad (7.7)$$

By calculating the kinetic energy and the force function, the equations of motion have been determined

$$\frac{1}{m}Q_\rho = \ddot{\rho} - \rho(\dot{\theta} + \dot{v})^2 + \frac{d\Phi}{dt} - (\dot{\theta} + \dot{v})\frac{\partial\Phi}{\partial\theta} \quad (7.8)$$

$$\frac{1}{m}Q_\theta = \frac{d}{dt}\left[\rho^2(\dot{\theta} + \dot{v}) + \rho\frac{\partial\Phi}{\partial\theta}\right] - 2\dot{\rho}\frac{\partial\Phi}{\partial\theta} + 2\rho(\dot{\theta} + \dot{v})\Phi \quad (7.9)$$

$$\frac{1}{m}Q_z = \ddot{z} \quad (7.10)$$

7.3. Numerical applications according to known problems of analytical mechanics

In this chapter, two of the most well-known problems of analytical mechanics were considered: the two-body problem and the restricted three-body problem. In this regard, the equations of motion between the bodies in inertial reference frames were defined using the Lagrange formalism.

Numerical simulations for both cases were conducted using the Matlab/Simulink simulation environment. Regarding the motion of two bodies in space relative to an inertial reference frame, the motion of the two bodies was obtained in an inertial reference frame with respect to the barycenter, as well as the motion of one body relative to the other.

One of the most renowned problems in classical dynamics is the restricted three-body problem, which holds practical significance in celestial mechanics. By obtaining the equations of motion, the relative motion of the asteroid and the Jacobi constant were simulated in this case.

7.4. Motion around an orbital station

In this subsection, the aim is to obtain numerical simulations resulting from the relative motion between a satellite and an orbital station when a specific type of orbit is defined, in this case, a circular orbit. The figure below illustrates the formulation of the problem for modeling the relative dynamics, where the target moves along a defined orbit.

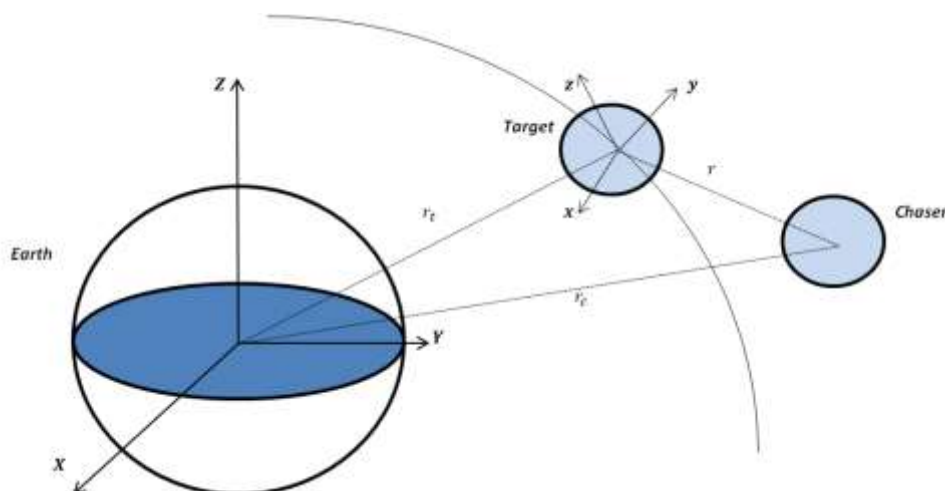


Figure 7.2 Coordinate system for a relative motion

As seen in Figure 7.2, the equations of motion will be determined by considering a non-inertial reference frame for the target and identifying the position of the chaser using cylindrical coordinates (r, θ, z) in the non-inertial reference frame and spherical coordinates (r_t, ν) in the inertial reference frame.

By applying the Lagrange formalism, the equations of motion have been obtained

$$\begin{cases} \ddot{r} + \frac{d\phi}{dt} - r(\dot{\nu} + \dot{\theta})^2 - (\dot{\nu} + \dot{\theta}) \frac{\partial \phi}{\partial \theta} = - \frac{GM(r+r_t \cos \theta)}{(r_t^2+r^2+2r_t r \cos \theta+z^2)^{\frac{3}{2}}} - \frac{Gm_t}{r^2} \\ \frac{d}{dt} [r^2(\dot{\nu} + \dot{\theta})] + r \frac{d}{dt} \left(\frac{\partial \phi}{\partial \theta} \right) - \dot{r} \frac{\partial \phi}{\partial \theta} + r(\dot{\nu} + \dot{\theta}) \phi = \frac{GM r_t r \sin \theta}{(r_t^2+r^2+2r_t r \cos \theta+z^2)^{\frac{3}{2}}} \\ \ddot{z} = - \frac{GMz}{(r_t^2+r^2+2r_t r \cos \theta+z^2)^{\frac{3}{2}}} \end{cases} \quad (7.11)$$

Given the known mathematical relationships and properties of a circular orbit, it is observed that

$$\frac{1}{\omega} \sqrt{\frac{GM}{r_t^3}} = 1 \quad (7.12)$$

Using this property and considering that the trajectory of the motion is of the form $r = r(\theta)$, the equation of relative motion has been obtained by integrating the relationship below

$$\frac{C_r - r^2}{r^2} \frac{d^2(\frac{1}{r})}{d\theta^2} + 2r(C_r - r^2) \left(\frac{d(\frac{1}{r})}{d\theta} \right)^2 + \frac{C_r^2}{r^3} = r + \frac{Gm_t}{\omega^2 r^2} \quad (7.13)$$

7.5. Study case

In this chapter, the objective is to obtain the relative motion of an astronaut with respect to an orbital station moving on a circular trajectory around the Earth. Several simulation scenarios are studied, depending on the initial distance between the astronaut and the station. The relative motion is obtained by integrating the equations (6.11), and the Matlab simulation environment is used for these case studies.

The aim is to simulate various relative motions of the astronaut with respect to the orbital station based on their initial distance.

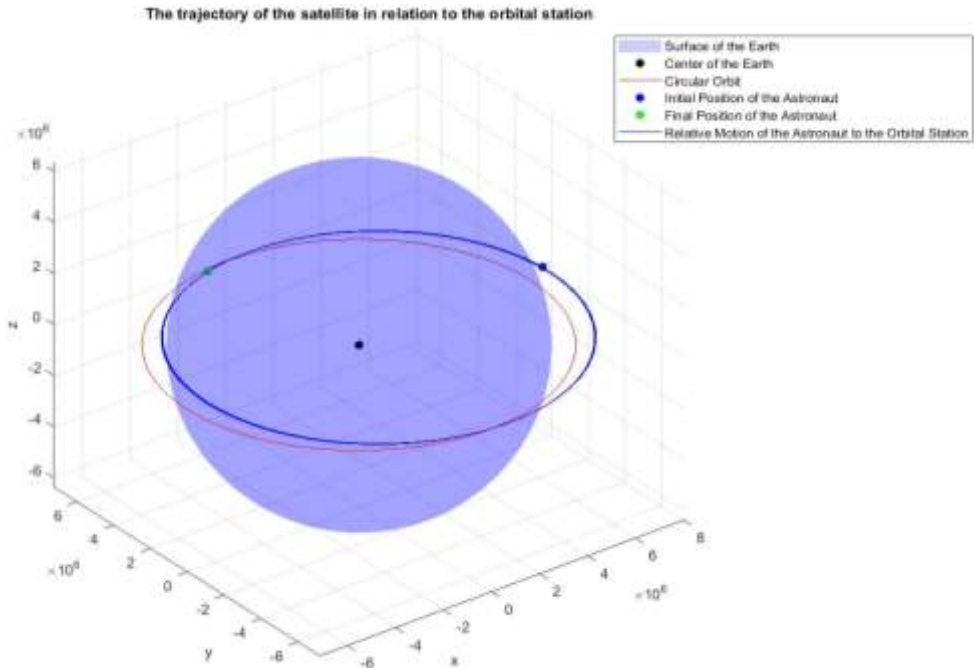


Figure 7.3 Initial distance between the astronaut and the orbital station of 1000km

As observed in the above figure, as the astronaut moves away from the station, their velocity and relative position become more closely aligned with the station. At this point, their motion appears to synchronize, as both follow the same orbital path around the Earth, and the gravitational forces acting upon them are relatively uniform, making their relative motion more predictable.

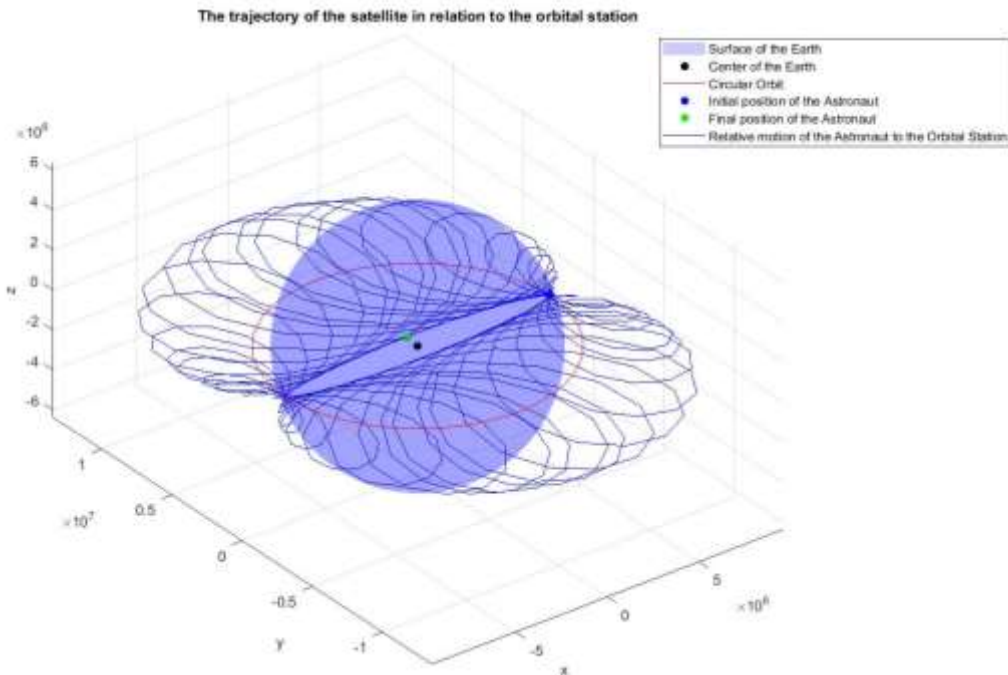


Figure 7.4 Initial distance between the astronaut and the orbital station of 3m

Regarding the behavior of the astronaut in the immediate vicinity of the orbital station, Figure 6.4, it is attributed to the effects of orbital mechanics and the laws of physics. Thus, their motion appears chaotic due to the variation of the $1/r$ function and various factors such as velocity differences, gravitational forces, and the inherent complexities of performing certain maneuvers.

This relative motion can cause the astronaut to experience erratic movement while adjusting their position and velocity to align with the station. Additionally, the small forces applied by the astronaut can have significant effects due to the absence of friction and the astronaut's reduced mass compared to that of the station.

7.6. Conclusions

In this chapter, the definitions of trajectories in inertial and non-inertial reference frames were discussed, using the Lagrange formalism. Numerical applications were also performed to solve well-known problems in analytical mechanics, namely the two-body problem and the restricted three-body problem. In this regard, it was observed that the use of the Lagrange formalism led to obtaining trajectories consistent with theoretical notions. The applied numerical methods allowed for a better understanding of the behavior of complex systems, such as multi-body systems interacting through gravitational forces.

Additionally, the relative motion of an astronaut around an orbital station was studied, with a focus on moments when the astronaut approaches the station as closely as possible. It was observed that the astronaut's motion becomes more complex near the station, influenced by velocity differences, gravitational forces, and the complexities associated with microgravity maneuvers.

By investigating this aspect, it was noted that the motion of the astronaut in the vicinity of the orbital station can be perceived as chaotic due to the complex interaction between relative forces and velocities.

The conclusions obtained in this chapter emphasize the importance of understanding and modeling relative motion in space systems, as well as the necessity of addressing the complexity of these interactions. These findings can guide the design and planning of future space missions, ensuring efficient navigation and maneuverability for astronauts around orbital stations.

Chapter 8

Conclusions and further developments

8.1. General conclusions

The main objective of this study was to investigate multi-body systems and mechanisms with applications in various fields. By analyzing the kinematics and dynamics of multi-body systems, fundamental concepts underlying the development and diversification of these mechanisms were identified and highlighted. Robotics has proven to be a highly relevant field in exploring new research directions in the dynamics and kinematics of multi-body systems, with implications in control, optimization, real-time simulation, path planning, reliability, and durability.

To simulate the complex motions of interconnected multi-body systems through kinematic joints and force elements, the importance of defining the nonlinear equations of motion was emphasized. Multi-body dynamics methods have become increasingly widespread, versatile, and reliable in simulating various engineering problems involving the dynamics of complex mechanisms. Additionally, fundamental aspects of kinematic and dynamic analysis for multi-body systems were presented, including the definition of general equations of motion using generalized Cartesian coordinates and the Lagrangian method. The importance of analyzing multi-body systems was emphasized because an increasing number of industrial applications rely on this precise analysis, especially regarding the forces acting on moving systems and mechanisms.

In the third chapter, the kinematic and dynamic model of a six-degree-of-freedom serial manipulator was developed, and simulations were conducted using Matlab and RobotStudio environments. Solutions for forward and inverse kinematics were obtained using Denavit-Hartenberg parameters and an iterative calculation procedure. A mathematical model for the inverse kinematics of the serial manipulator was developed, considering variable constraints and analytically determining the Jacobian. Further developments focused on improving the control of the end effector of the serial manipulator, which operates with flexible elements and relies on the presented kinematic and dynamic model. A trajectory of the robot's end effector was simulated to track the variation of the six joint angles and the mechanical torques acting on them. The obtained results validated the described mathematical model, and the trajectory obtained in the Matlab simulation environment was compared with the one obtained in the RobotStudio environment.

In the fourth chapter, the closed-form dynamic equations for a six-degree-of-freedom parallel manipulator were presented, using the Lagrangian formalism. The algorithm was implemented in the Matlab simulation environment, and the numerical results were studied to validate the presented dynamic formulation. The simulation results demonstrated the possibility of explicitly deriving the dynamic equations in the task space for a six-degree-of-freedom manipulator, thereby obtaining the actuation forces on the mobile platform's actuators.

In the fifth chapter, two simulation cases of vertical landing of a quadcopter on a Stewart platform were presented, utilizing the backstepping control method, which showed a high capacity for controlling the position angles in the presence of various disturbances. The relative motion of the vehicle with respect to the mobile platform was analyzed, considering the six degrees of freedom of each model. The simulations revealed that as the platform elevation becomes more dynamic, the control of the quadcopter's attitude becomes more challenging, stabilizing over a longer period of time.

Chapter six aimed at experimental analysis regarding the landing of an aerial vehicle attached to the end effector of an ABB7600-500 robot on a Stewart platform. Thus, the theoretical model described in the previous chapters was validated.

In the seventh chapter of the work, the relative motion simulation between an astronaut and an orbital station on a circular orbit was addressed, presenting the formulation of the problem of modeling relative dynamics. Considering the importance of adjusting trajectory and velocity for astronaut-station synchronization, it was noted that the trajectory becomes chaotic, leading to numerical instabilities due to the variation of the function $1/r$.

In conclusion, the results and simulations presented in this study can serve as a basis for further developments in the design and performance analysis of multi-body systems, including serial and parallel manipulators, quadcopters, and spacecraft. Further advancements can be made in control, algorithms, and dynamic modeling to improve the performance and efficiency of these systems. Aspects such as actuator stiffness, effects of uncertainties, and landing site incidence on trajectories and vehicle control can also be considered.

8.2. Original contributions

This paper represents a significant contribution to the study of multibody systems and mechanisms with diverse applications. The main objective of this study was to explore in-depth multibody systems and mechanisms, with a focus on analyzing the kinematics and dynamics of these complex systems. Through detailed analysis of these fundamental aspects, essential concepts underlying the development and diversification of multi-body mechanisms were highlighted and understood. Several original contributions were achieved and emphasized through the research efforts, including:

- Development of an original inverse kinematics model for the ABB7600 robotic arm, using Denavit-Hartenberg parameters. This model underwent rigorous verification and validation processes, representing a significant contribution to the analysis of serial manipulator kinematics. Additionally, within the same chapter, a dynamic model of the robot was developed using the Lagrangian formalism. This model provides a detailed description of the dynamic behavior of the robot and represents an original contribution to the understanding and simulation of complex mechanisms.
- Obtaining a dynamic model of the Stewart platform PS-6TL-1500 using the Lagrangian formalism. The model included the simulation of forces acting on the actuators, considering factors such as the payload mass of the upper platform, motion along the three axes and attitude angles.
- Development of a landing model for a quadcopter on a Stewart platform using the backstepping control method. This model underwent verification and validation processes, taking into consideration the movement of the Stewart platform. The original contribution lies in the innovative approach to precise control of position angles in the presence of disturbances.
- Experimental analysis validating the fixed-point landing model of an aerial vehicle on a mobile platform.
- Obtaining a dynamic model of the relative motion between an astronaut and an orbital station on a circular orbit. The dynamic model followed the Lagrangian formalism, using spherical and cylindrical coordinates. Specific aspects of the circular orbit were considered and the simulation was performed based on the initial positions and velocities of the astronaut and the orbital station.

These contributions open new research directions in the fields of control, algorithms and dynamic modeling, with the aim of improving the performance and efficiency of these complex systems. Furthermore, aspects such as actuator stiffness, uncertainties, and the impact of landing sites on trajectories and vehicle control can be integrated and considered.

8.3. Future research directions

Based on the contributions presented in this paper, there are several future research directions that can be further explored to develop and deepen the field of multi-body systems and mechanisms. These directions include, but are not limited to:

1. **Advanced control of multi-body systems:** Improving and developing advanced control algorithms for serial and parallel manipulators, quadcopters, and spacecraft can be a promising direction. The use of techniques such as adaptive control, predictive control, or machine learning can contribute to enhancing the performance and precision of multi-body systems.

2. **Modeling and analysis of uncertainties:** Considering uncertainties in the modeling and analysis of multibody systems can be an important aspect to achieve more realistic results. Incorporating uncertainties in the parameters of mechanisms, actuators, and the environment can contribute to developing more robust models and a better understanding of system behavior under real conditions.

3. **Integration of flexibility and deformations:** In many practical applications, mechanisms involve flexible elements or undergo deformations during operation. Studying the interaction between the rigidity and flexibility of mechanical components can provide new insights into the analysis and control of multi-body systems. Developing suitable methods and techniques for modeling and simulating deformations and flexible behavior of mechanisms can be considered a new research direction.

4. **Optimization of multibody system performance:** Optimization can focus on aspects such as minimizing efforts or vibrations, maximizing motion precision and efficiency, reducing energy consumption, or maximizing system stability. Techniques such as genetic algorithm-based optimization, artificial intelligence-based optimization, or multi-objective optimization can be employed to achieve better results in the design and control of multibody systems.

5. **Extension to specific applications:** Research can be oriented towards specific domains where multibody systems and mechanisms have significant applications. For example, in the medical field, the development and analysis of multi-body systems for assistive robots or simulating human movements can be of great interest. In the domain of assembly or manufacturing robots, optimizing multibody systems to perform complex and precise operations can be an important research direction.

These are just a few of the future research directions that can be further explored based on the contributions and results presented in this paper. By exploring these directions, progress can be made in the development and practical application of multibody systems and mechanisms, opening up new opportunities in various fields.

Selective Bibliography

- [2] Kurfess, T. R., Robotics and Automation Handbook, CRC Press, 1st Edition, 2004.
- [5] Thien, V. N., „Thesis for degree of Doctor of Philosophy ”Contribution to Kinematic and Dynamic Study of Rigid Bodies”,” București, 2018.
- [19] Kevin M. Lynch, Frank C. Park, Modern Robotics. Mechanics, Planning and Control, Cambridge University Press, 2017.
- [25] Gavin, Henri P., „Generalized Coordinates, Lagrange's Equations and Constraints,” Department of Civil and Environmental Engineering Duke University, Durham, USA, 2016.
- [32] Lee T., „Global Formulations of Lagrangian and Hamiltonian Dynamics of Manifolds,” *Springer International Publishing*, pp. 273-311, 2018.
- [33] Stroe Ion, „Trajectories in non-inertial frames,” *Scientific Bulletin of University „Politehnica” of Bucharest*, pp. 21-28, 2010.
- [38] Seemal Asif, Philip Webb, „Kinematics Analysis of 6-DOF articulates robot with spherical wrist,” *Mathematical Problems in Engineering* , vol. 2021, nr. 6647035, p. 11, 2021.
- [43] Feifan He, Qingju Huang, „Time-Optimal Trajectory Planning of 6-dof Manipulator Based on Fuzzy Control,” *Actuators*, vol. 11, 16 noiembrie 2022.
- [44] Phan Bui Khoi, Ha Thanh Hai, Hoang Vinh Sinh, „Dynamic Analysis of Robot In Machining,” *International Journal of Mechanical and Production Engineering Reserach and Development* , vol. 10, nr. 1, pp. 223-236, 2020.
- [48] Charles C. Nguyen, Sami S. Antrazi, „Experimental Study of Trajectory Planning and Control of a High Precision Robot Manipulator” Goddard Space Flight Center (NASA), Greenbelt, Maryland, 1991.
- [60] Francesco Ruscelli, Arturo Laurenzi, Nikos G. Tsagarakis, Enrico Mingo Hoffman, „Horizon: A Trajectory Optimization Framework for Robotic Systems,” *Frontiers in Robotics and AI*, vol. 9, 13 iulie 2022.
- [70] **Sandra-Elena Nichifor**, Ion Stroe, Mihaela-Luminița Costea, Florin Costache, „Vertical Take Off Landing Of UAV On Stewart Platform,” în *19th International Conference of Numerical Analysis and Applied Mathematics (ICNAAM 2021)*, Rodos, Grecia, 2021.
- [71] Ștefan Eugen Stoian, Dragoș Daniel Ion-Guță, **Sandra Elena Nichifor**, Florentin Șperlea, Achim Ioniță, „TWQH Attitude Control Experiments on Horizon Ground Simulator and Flight Test,” *INCAS BULLETIN*, vol. 12, nr. 1, pp. 183-198, 2020.
- [72] Florin Costache, **Sandra-Elena Nichifor**, Mihaela-Luminița Costea, Achim Ioniță, „Automatic approach procedure of a flying vehicle on a mobile platform using backstepping controller,” *INCAS BULLETIN*, vol. 14, nr. 4, pp. 51-62, december 2022.
- [73] Florin Costache, **Sandra-Elena Nichifor**, Nicolae Apostolescu, Mihaela-Luminița Costea, Achim Ioniță, „Real-Time interaction between an ABB 7600 Robot and a Stewart Platform,” în *19th International Conference of Numerical Analysis and Applied Mathematics (ICNAAM 2021)*, Rodos, Grecia, 2021.